Hindawi
Discrete Dynamics in Nature and Society
Volume 2023, Article ID 7710701, 30 pages
https://doi.org/10.1155/2023/7710701

Research Article

The Diffusion-Driven Instability for a General Time-Space Discrete Host-Parasitoid Model

Xuetian Zhang and Chunrui Zhang

School of Science, Northeast Forestry University, Harbin 150040, China

Correspondence should be addressed to Xuetian Zhang; xuetianmath@163.com and Chunrui Zhang; math@nefu.edu.cn

Received 7 November 2022; Revised 9 March 2023; Accepted 14 March 2023; Published 6 April 2023

Academic Editor: Jesus M. Munoz-Pacheco

In this paper, we consider a general time-space discrete host-parasitoid model with the periodic boundary conditions. We analyzed and obtained some usual conditions, such as Turing instability occurrence, Flip bifurcation occurrence, and Neimark-Sacker bifurcation occurrence. We also find several multiple bifurcation phenomena, such as 1 : 2 Resonance, Neimark-Sacker-Flip bifurcation, Neimark-Sacker-Neimark-Sacker bifurcation, Neimark-Sacker-Flip-Flip bifurcation, induced by diffusion. In a modified Nicholson-Bailey model, employing the mutual interference and diffusive interaction as bifurcation parameters, there appear route from standing Turing instability to multiple bifurcations by changing diffusive parameters. Some numerical simulations of the modified Nicholson-Bailey model support these corollaries.

1. Introduction

The achievements of physics, chemistry, ecology, and other disciplines have considerably contributed to the development of natural disciplines, the development and progress of which cannot be achieved without mathematical models. Since some objects in nature are not only changing with time but also have a diffusion phenomenon in space, numerous mathematical models are combined with time and space, and we can call this type of models reaction-diffusion models. In recent decades, the reaction-diffusion model has been widely used and numerous experts and scholars have used it to study the dynamic behavior of various organisms in nature [1–11], and the results of these studies have played a positive role in environmental protection and governance.

The reaction-diffusion models can be further subdivided into continuous reaction-diffusion models [12–15] and discrete reaction-diffusion models [16, 17]. In biomathematical models, continuous models can be used to describe organisms that are based on a large amount of data, but for organisms in which many movements and changes occur in discrete forms and the data collected and recorded are also in discrete forms; constructing discrete models to describe them will be more in line with objective reality such as host-parasitoid models.

In recent years, many scientists, ecologists, and biologists have studied and analyzed the relationship between hosts and parasitoids [18–26]. For some hosts of endangered species, specific parasite reduction is likely to lead to the immediate extinction of the host species. The conservation of biodiversity in nature is closely related to the protection of some specific parasites. Therefore, the research results of scholars and scientists on the relationship between host parasites are crucial for the protection of endangered hosts and the maintenance of biodiversity. According to [27], we know that for insects, continuous-time models are generally used to model populations with overlapping generations and year-round reproduction, discrete-time models are more appropriate for populations in temperate regions of the world that have nonoverlapping generations and reproduce in discrete pulses determined by seasons. For hosts and parasitoids, adult hosts lay eggs and hatch larvae in the spring and host larvae overwinter in the pupal stage and become adult hosts the following year. Adult hosts die after the emergence of host larvae, and there is no overlap

between generations. The female parasitoid emerges in the spring and lays eggs inside the host larvae when it searches for and encounters them. After the parasitoid's eggs hatch into parasitoid larvae, they will use the host larvae as a food source, which will result in the death of the parasitized host larvae. These parasitoid larvae will also overwinter in the pupal stage and become adult parasitoids the following year. Adult parasitoids die after the emergence of parasitoid larvae, and there is no overlap between generations, see Figure 1. There is a clear intergenerational relationship between both host and parasitoid, so constructing a discrete model to describe them is more in line with objective reality. Readers interested in more host-parasitoid models are referred to [28–34] and references therein. Considering that both host and parasitoid have self-diffusion behavior in space, we will investigate and analyze a general time-space discrete host-parasitoid model in this paper.

Usually, in a continuous and a discrete medium, the propagation of small difference and the taking over of steady states are very different. For example, Flip bifurcation cannot occur in continuous dynamics, and hence, the chaos phenomenon usually appears in discrete model easily.

The rest of the paper is organized as follows: A general time-space discrete host-parasitoid model with periodic boundary conditions is given in Section 2, which is the main object of our study. Then, we analyze the stability of the host-parasitoid model in the absence of diffusion case by using the Jury criterion and analyzing the characteristic roots of the characteristic equations, and obtain the stability condition and a Neimark-Sacker bifurcation condition in Section 3.1. Combining the periodic boundary conditions and the eigenvalues of the nonlinear discrete elliptic equations, we transform a linear system of partial difference into a linear system of difference equations by using the corresponding eigenfunctions to do inner products, and the stability of the solutions between them is mutually implied.

Then, we analyze the stability of the transformed linear system of difference equations, and thus, obtain various instability conditions and various critical conditions of the original system caused by diffusion-driven, such as Turing instability, Neimark-Sacker instability, Neimark-Sacker-Turing instability, Flip bifurcation, Neimark-Sacker bifurcation, 1 : 2 Resonance, Neimark-Sacker-Flip bifurcation, Neimark-Sacker-Neimark-Sacker bifurcation, and Neimark-Sacker-Flip-Flip bifurcation, see Section 3.2. We apply the obtained conclusions to a specific modified Nicholson-Bailey model, then we obtain the corresponding corollaries in Sections 4.1, 4.2, and the corresponding numerical simulation in Sections 4.3.1, 4.3.2, where we use a random matrix combined with boundary conditions to assign initial values in Section 4.3.2. Finally, the paper ends with an overall detailed summary in Section 5.

2. A General Time-Space Discrete Host-Parasitoid Model

According to [35], a model describing host-parasitoid dynamics in discrete-time is given by

$$\begin{cases} H_{n+1} = \mathrm{RH}_n f\left(RH_n, P_n\right), \\ P_{n+1} = \mathrm{kRH}_n\left[1 - f\left(RH_n, P_n\right)\right]. \end{cases} \tag{1}$$

H_n and P_n represent the densities of adult hosts and adult parasitoids in year n, respectively. The host is parasitized by parasitoids during the larval stage, RH_n represents the density of parasitoid larvae, where $R > 1$ denotes the number of viable eggs produced by each adult host. Hosts in the larval stage can be divided into two groups, one is parasitized and the other is not parasitized, and the function $0 \le f\left(RH_n, P_n\right) \le 1$, a continuously differentiable function, represents the proportion of this part that is not parasitized, we can refer to it as the escape response. In accordance with the biological significance, the escape response $f\left(RH_n, P_n\right)$ is a monotonically decreasing function with respect to P_n. Finally, it is important to point out that $RH_n f\left(RH_n, P_n\right)$ is the density of unparasitized host larvae, which will become adult hosts in the next year, $RH_n\left[1 - f\left(RH_n, P_n\right)\right]$ is the density of parasitized host larvae, and k parasitoid larvae will hatch in the body of each parasitized host larva. For further information, please read reference [36–39].

Considering that both parasitoids and hosts can spread in space, we define a discrete space of $(m+2) \times (m+2)$, $m \in \mathbb{Z}^+$ and rewrite (1) into the following form:

$$\begin{cases} H_{n+1}(i,j) = RH_n(i,j) f\left(RH_n(i,j), P_n(i,j)\right) \\ +d_1 \nabla^2 H_n(i,j), \\ P_{n+1}(i,j) = kRH_n(i,j)\left[1 - f\left(RH_n(i,j), P_n(i,j)\right)\right] \\ +d_2 \nabla^2 P_n(i,j), \end{cases} \tag{2}$$

with the periodic boundary conditions

$$\begin{aligned} H_n(i,0) &= H_n(i,m), H_n(i,1) = H_n(i,m+1), \\ H_n(0,j) &= H_n(m,j), H_n(1,j) = H_n(m+1,j), \\ P_n(i,0) &= P_n(i,m), P_n(i,1) = P_n(i,m+1), \\ P_n(0,j) &= P_n(m,j), P_n(1,j) = P_n(m+1,j), \end{aligned} \tag{3}$$

for $i, j, n \in \mathbb{Z}^+$ and $1 \le i, j \le m$, where the host and parasitoid densities in the lattice point (i, j) at time n are defined as $H_n(i,j)$ and $P_n(i,j)$, respectively. d_1 and d_2 represent the self-diffusion coefficients of the host and parasitoid, respectively, and both are positive real numbers. The meaning of the remaining parameters is the same as in (1).

The discrete Laplacian operator is defined as

$$\begin{cases} \nabla^2 H_n(i,j) = H_n(i+1,j) + H_n(i,j+1) + H_n(i-1,j) \\ +H_n(i,j-1) - 4H_n(i,j), \\ \nabla^2 P_n(i,j) = P_n(i+1,j) + P_n(i,j+1) + P_n(i-1,j) \\ +P_n(i,j-1) - 4P_n(i,j). \end{cases} \tag{4}$$

The next part of our main research content is to study the dynamic properties of (2) and (3).

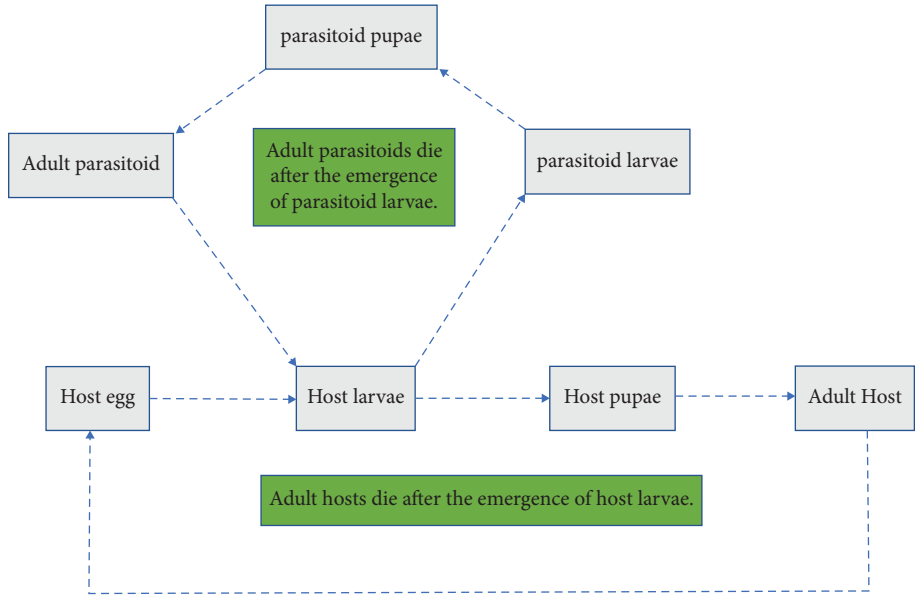

Figure 1: Host and parasitoid life cycle.

3. Bifurcation Induced by Diffusion of the Host-Parasitoid Model

3.1. Stability Analysis of the Host-Parasitoid Model in the Absence of Diffusion. In the absence of self-diffusion, the system (2) and (3) will degenerate into (1). According to [27], we can obtain its positive equilibrium point (H^*P^*) satisfying $Rf(RH^*, P^*) = 1$ and $P^* = k(R-1)H^*$. Let $\overline{H}_n = H_n - H^*, \overline{P}_n = P_n - P^*$, the (1) can be rewritten as

$$\begin{cases} \overline{H}_{n+1} + H^* = R(\overline{H}_n + H^*) f(R(\overline{H}_n + H^*), (\overline{P}_n + P^*)), \\ \overline{P}_{n+1} + P^* = kR(\overline{H}_n + H^*)[1 - f(R(\overline{H}_n + H^*), (\overline{P}_n + P^*))]. \end{cases} \tag{5}$$

Then, we linearize the system (5) to obtain the following linear system:

$$\begin{pmatrix} \overline{H}_{n+1} \\ \overline{P}_{n+1} \end{pmatrix} = A \begin{pmatrix} \overline{H}_n \\ \overline{P}_n \end{pmatrix}, A = \begin{pmatrix} a_1 & a_2 \\ b_1 & b_2 \end{pmatrix}. \tag{6}$$

The elements in the Jacobi matrix A are as follows:

$$\begin{aligned} a_1 &= 1 + RH^* \frac{\partial f(RH_n, P_n)}{\partial H_n}\bigg|_{H_n=H^*, P_n=P^*}, \\ a_2 &= RH^* \frac{\partial f(RH_n, P_n)}{\partial P_n}\bigg|_{H_n=H^*, P_n=P^*}, \\ b_1 &= k(R-1) - kRH^* \frac{\partial f(RH_n, P_n)}{\partial H_n}\bigg|_{H_n=H^*, P_n=P^*}, \\ b_2 &= -kRH^* \frac{\partial f(RH_n, P_n)}{\partial P_n}\bigg|_{H_n=H^*, P_n=P^*}. \end{aligned} \tag{7}$$

The characteristic equation of (6) is

$$\lambda^2 + b\lambda + c = 0, \tag{8}$$

where $b = -(a_1 + b_2), c = a_1 b_2 - a_2 b_1$, the eigenvalues are given by

$$\lambda_{1,2} = \frac{-b \pm \sqrt{b^2 - 4c}}{2}. \tag{9}$$

According to the Jury stability criterion, the system (5) is stable at the origin if and only if the following condition holds:

$$\begin{cases} 1 + b + c > 0, \\ 1 - b + c > 0, \\ c < 1, \end{cases} \tag{10}$$

which implies that the eigenvalues of the Jacobian matrix A are all inside the unit circle. Therefore, we can obtain the following theorem:

Theorem 1. *System (1) is asymptotically stable at positive equilibrium (H^*, P^*) if and only if (10)) holds.*

A Neimark-Sacker bifurcation occurs when a pair of conjugate complex eigenvalues of the matrix A crosses the unit circle. For generality of consequences we set ρ, any one

parameter in system (1), to be the Neimark-Sacker bifurcation parameter and set ρ^* to be the critical value such that $|b|<2$ and $c=1$ at $\rho=\rho^*$. If ρ is valued near ρ^*, (9) can be written in the form of a pair of conjugate complex roots as follows:

$$\lambda_{1,2}=\frac{-b(\rho)}{2}\pm\frac{\sqrt{4c(\rho)-b^2(\rho)}}{2}i, \tag{11}$$

where $|b(\rho^*)|<2$, $c(\rho^*)=1$. Then, we have $\|\lambda_{12}\|^2=\mathrm{c}(\rho)$. If the following transversality condition (12) is satisfied, the system (5) undergoes a Neimark-Sacker bifurcation at $\rho=\rho^*$.

$$\left.\frac{\partial \mathrm{c}(\rho)}{\partial\rho}\right|_{\rho=\rho^*}\neq 0. \tag{12}$$

Therefore, we can obtain the following theorem:

Theorem 2. *If $|b(\rho^*)|<2, c(\rho^*)=1$ and the transversality condition (12) are satisfied, the system (1) undergoes a Neimark-Sacker bifurcation at $\rho=\rho^*$.*

3.2. Diffusion-Driven Instability Analysis of the Host-Parasitoid Model. To facilitate the study of the system (2) and (3), we first consider the following two lemmas:

We attach periodic bounds to $u_{i,j}, v_{i,j}$ as follows:

$$\begin{aligned}
u_{i,0}&=u_{i,m}, u_{i,1}=u_{i,m+1},\\
u_{0,j}&=u_{0,m}, u_{1,j}=u_{m+1,j},\\
v_{i,0}&=v_{i,m}, v_{i,1}=v_{i,m+1},\\
v_{0,j}&=v_{0,m}, v_{1,j}=v_{m+1,j},
\end{aligned} \tag{13}$$

where $i,j,n\in\mathbb{Z}^+$, $1\le i,j\le m$, and default $u_{i,j}v_{l,s}=v_{l,s}u_{i,j}$ holds $(i,j,l,s\in\mathbb{Z}^+, 1\le i,j,l,s\le m)$, then we have the first lemma as follows:

Lemma 1. *If (13) holds, we have*

$$\sum_{i,j=1}^{m}\mathrm{u}_{i,j}\nabla^2 v_{i,j}=\sum_{i,j=1}^{m}v_{i,j}\nabla^2 u_{i,j}. \tag{14}$$

Proof. We can make some definitions as follows:

$$\begin{aligned}
U_{i,j}(1)&=\mathrm{u}_{i,j}v_{i+1,j}, V_{i,j}(1)=v_{i,j}u_{i+1,j},\\
U_{i,j}(2)&=\mathrm{u}_{i,j}v_{i,j+1}, V_{i,j}(2)=v_{i,j}u_{i,j+1},\\
U_{i,j}(3)&=\mathrm{u}_{i,j}v_{i,j-1}, V_{i,j}(3)=v_{i,j}u_{i,j-1},\\
U_{i,j}(4)&=\mathrm{u}_{i,j}v_{i-1,j}, V_{i,j}(4)=v_{i,j}u_{i-1,j}.
\end{aligned} \tag{15}$$

Then, we can get (16) and (17).

$$\begin{aligned}
V_{0,j}(1)&=v_{0,j}u_{1,j}=v_{m,j}u_{m+1,j}=V_{m,j}(1),\\
V_{i,0}(2)&=v_{i,0}u_{i,1}=v_{i,m}u_{i,m+1}=V_{i,m}(2),\\
V_{i,m+1}(3)&=v_{i,m+1}u_{i,m}=v_{i,1}u_{i,0}=V_{i,1}(3),\\
V_{m+1,j}(4)&=v_{m+1,j}u_{m,j}=v_{1,j}u_{0,j}=V_{1,j}(4).
\end{aligned} \tag{16}$$

In fact, $U_{i,j}$ also satisfies periodic boundary conditions, but given that the next proof uses only periodic properties of $V_{i,j}$, we will not repeat $U_{i,j}$ here.

$$\begin{aligned}
U_{i,j}(1)&=u_{i,j}v_{i+1,j}=v_{i+1,j}u_{i,j}=V_{i+1,j}(4),\\
U_{i,j}(2)&=u_{i,j}v_{i,j+1}=v_{i,j+1}u_{i,j}=V_{i,j+1}(3),\\
U_{i,j}(3)&=u_{i,j}v_{i,j-1}=v_{i,j-1}u_{i,j}=V_{i,j-1}(2),\\
U_{i,j}(4)&=u_{i,j}v_{i-1,j}=v_{i-1,j}u_{i,j}=V_{i-1,j}(1).
\end{aligned} \tag{17}$$

Finally, we have

$$\begin{aligned}
&\sum_{i,j=1}^{m}u_{i,j}\nabla^2 v_{i,j}\\
&=\sum_{i,j=1}^{m}\left(U_{i,j}(1)+U_{i,j}(2)+U_{i,j}(3)+U_{i,j}(4)\right)-4\sum_{i,j=1}^{m}u_{i,j}v_{i,j}\\
&=\sum_{i,j=1}^{m}V_{i+1,j}(4)+\sum_{i,j=1}^{m}V_{i,j+1}(3)+\sum_{i,j=1}^{m}V_{i,j-1}(2)+\sum_{i,j=1}^{m}V_{i-1,j}(1)\\
&\quad-4\sum_{i,j=1}^{m}u_{i,j}v_{i,j}\\
&=\sum_{i=2}^{m}\left(\sum_{j=1}^{m}V_{i,j}(4)\right)+\sum_{j=1}^{m}V_{m+1,j}(4)+\sum_{j=2}^{m}\left(\sum_{i=1}^{m}V_{i,j}(3)\right)\\
&\quad+\sum_{i=1}^{m}V_{i,m+1}(3)+\sum_{j=1}^{m-1}\left(\sum_{i=1}^{m}V_{i,j}(2)\right)+\sum_{i=1}^{m}V_{i,0}(2)\\
&\quad+\sum_{i=1}^{m-1}\left(\sum_{j=1}^{m}V_{i,j}(1)\right)+\sum_{j=1}^{m}V_{0,j}(1)-4\sum_{i,j=1}^{m}u_{i,j}v_{i,j}\\
&=\sum_{i=2}^{m}\left(\sum_{j=1}^{m}V_{i,j}(4)\right)+\sum_{j=1}^{m}V_{1,j}(4)+\sum_{j=2}^{m}\left(\sum_{i=1}^{m}V_{i,j}(3)\right)\\
&\quad+\sum_{i=1}^{m}V_{i,1}(3)+\sum_{j=1}^{m-1}\left(\sum_{i=1}^{m}V_{i,j}(2)\right)+\sum_{i=1}^{m}V_{i,m}(2)\\
&\quad+\sum_{i=1}^{m-1}\left(\sum_{j=1}^{m}V_{i,j}(1)\right)+\sum_{j=1}^{m}V_{m,j}(1)-4\sum_{i,j=1}^{m}u_{i,j}v_{i,j}\\
&=\sum_{i,j=1}^{m}\left(V_{i,j}(1)+V_{i,j}(2)+V_{i,j}(3)+V_{i,j}(4)\right)-4\sum_{i,j=1}^{m}u_{i,j}v_{i,j}\\
&=\sum_{i,j=1}^{m}v_{i,j}\nabla^2 u_{i,j}.
\end{aligned} \tag{18}$$

□

The second lemma is to consider the eigenvalue problem of the following equation:

$$\nabla^2 X^{i,j} + \lambda X^{i,j} = 0, \tag{19}$$

with the periodic boundary conditions

$$\begin{aligned} X^{0,j} &= X^{m,j}, X^{1,j} = X^{m+1,j}, \\ X^{i,0} &= X^{i,m}, X^{i,1} = X^{i,m+1}. \end{aligned} \tag{20}$$

Lemma 2. *If (19) and (20) hold, we have*

$$\lambda_{l,s} = k_{l,s}^2 = 4\left(\sin^2\frac{(l-1)\pi}{m} + \sin^2\frac{(s-1)\pi}{m}\right), \tag{21}$$

where $l, s \in \mathbb{Z}^+$ and $1 \le l, s \le m$.

Proof. According to the method in [40], we let $X^{i,j} = x^i y^j$ $(x \ne 0, y \ne 0)$ and bring it into (19). Then, we have

$$x^{i+1}y^j + x^i y^{j+1} + x^i y^{j-1} + x^{i-1}y^j - 4x^i y^j + \lambda x^i y^j = 0, \tag{22}$$

which implies

$$\lambda = -\left(x + y + y^{-1} + x^{-1} - 4\right). \tag{23}$$

We can get $x^m = 1, y^m = 1$ by (20), so x and y can be written as follows:

$$\begin{aligned} x_l &= e^{2(l-1)\pi/mi}, \\ y_s &= e^{2(s-1)\pi/mi}, \end{aligned} \tag{24}$$

where $i = \sqrt{-1}, l, s \in \mathbb{Z}^+$ and $1 \le l, s \le m$.

By putting (24) into (23), we can obtain the eigenvalues of equation (19) as follows:

$$\lambda_{l,s} = k_{l,s}^2 = 4\left(\sin^2\frac{(l-1)\pi}{m} + \sin^2\frac{(s-1)\pi}{m}\right). \tag{25}$$

The corresponding characteristic function is denoted as $X_{l,s}^{i,j}$. □

Referring to the approach in the literature [1, 2, 16, 17], we started to study the stability of the system (2) and (3). Let $\overline{H}_n(i,j) = H_n(i,j) - H^*, \overline{P}_n(i,j) = P_n(i,j) - P^*$, then (2) can be rewritten as follows:

$$\begin{cases} \overline{H}_{n+1}(i,j) + H^* = R\left(\overline{H}_n(i,j) + H^*\right) \\ \times f\left(R\left(\overline{H}_n(i,j) + H^*\right), \left(\overline{P}_n(i,j) + P^*\right)\right) \\ +d_1\nabla^2\left(\overline{H}_n(i,j) + H^*\right), \\ \overline{P}_{n+1}(i,j) + P^* = kR\left(\overline{H}_n(i,j) + H^*\right) \\ \times\left[1 - f\left(R\left(\overline{H}_n(i,j) + H^*\right), \left(\overline{P}_n(i,j) + P^*\right)\right)\right] \\ +d_2\nabla^2\left(\overline{P}_n(i,j) + P^*\right). \end{cases} \tag{26}$$

Then, we linearize the system (26) to obtain the following linear system:

$$\begin{aligned} \begin{pmatrix} \overline{H}_{n+1}(i,j) \\ \overline{P}_{n+1}(i,j) \end{pmatrix} &= \begin{pmatrix} a_1 & a_2 \\ b_1 & b_2 \end{pmatrix}\begin{pmatrix} \overline{H}_n(i,j) \\ \overline{P}_n(i,j) \end{pmatrix} \\ &+ \begin{pmatrix} d_1 & 0 \\ 0 & d_2 \end{pmatrix}\begin{pmatrix} \nabla^2\overline{H}_n(i,j) \\ \nabla^2\overline{P}_n(i,j) \end{pmatrix}. \end{aligned} \tag{27}$$

Clearly, $\overline{H}_n(i,j)$, $\overline{P}_n(i,j)$, and $X_{l,s}^{i,j}$ all satisfy periodic boundary conditions, and by Lemmas 1 and 2, we have

$$\begin{cases} \sum_{i,j=1}^{m} X_{l,s}^{i,j}\nabla^2\overline{H}_n(i,j) = \sum_{i,j=1}^{m} \overline{H}_n(i,j)\nabla^2 X_{l,s}^{i,j} \\ = -k_{l,s}^2 \sum_{i,j=1}^{m} X_{l,s}^{i,j}\overline{H}_n(i,j), \\ \sum_{i,j=1}^{m} X_{l,s}^{i,j}\nabla^2\overline{P}_n(i,j) = \sum_{i,j=1}^{m} \overline{P}_n(i,j)\nabla^2 X_{l,s}^{i,j} \\ = -k_{l,s}^2 \sum_{i,j=1}^{m} X_{l,s}^{i,j}\overline{P}_n(i,j). \end{cases} \tag{28}$$

We get (29) by taking the inner product of the characteristic function $X_{l,s}^{i,j}$ with respect to (27).

$$\begin{cases} \sum_{i,j=1}^{m} X_{l,s}^{i,j}\overline{H}_{n+1}(i,j) = a_1\sum_{i,j=1}^{m} X_{l,s}^{i,j}\overline{H}_n(i,j) + a_2\sum_{i,j=1}^{m} X_{l,s}^{i,j}\overline{P}_n(i,j) \\ +d_1\sum_{i,j=1}^{m} X_{l,s}^{i,j}\nabla^2\overline{H}_n(i,j), \\ \sum_{i,j=1}^{m} X_{l,s}^{i,j}\overline{P}_{n+1}(i,j) = b_1\sum_{i,j=1}^{m} X_{l,s}^{i,j}\overline{H}_n(i,j) + b_2\sum_{i,j=1}^{m} X_{l,s}^{i,j}\overline{P}_n(i,j) \\ +d_2\sum_{i,j=1}^{m} X_{l,s}^{i,j}\nabla^2\overline{P}_n(i,j). \end{cases} \tag{29}$$

Let $\widetilde{H}_n = \sum_{i,j=1}^{m} X_{l,s}^{i,j}\overline{H}_n(i,j), \widetilde{P}_n = \sum_{i,j=1}^{m} X_{l,s}^{i,j}\overline{P}_n(i,j)$. By (28), we have

$$\begin{pmatrix} \widetilde{H}_{n+1} \\ \widetilde{P}_{n+1} \end{pmatrix} = B\begin{pmatrix} \widetilde{H}_n \\ \widetilde{P}_n \end{pmatrix}, B = \begin{pmatrix} a_1 - d_1k_{l,s}^2 & a_2 \\ b_1 & b_2 - d_2k_{l,s}^2 \end{pmatrix}. \tag{30}$$

Clearly, $\overline{H}_n(i,j) = \widetilde{H}_n X_{l,s}^{i,j}, \overline{P}_n(i,j) = \widetilde{P}_n X_{l,s}^{i,j}$ is a solution satisfying (27), so the stability of the solutions of systems (27) and (30) is mutually implied. We obtain the characteristic equation of (30) as follows:

$$\lambda^2 + p\left(k_{l,s}^2\right)\lambda + q\left(k_{l,s}^2\right) = 0, \tag{31}$$

where $p(k_{l,s}^2) = -(a_1 + b_2 - k_{l,s}^2(d_1 + d_2)), q(k_{l,s}^2) = d_1d_2k_{l,s}^4 - (d_1b_2 + d_2a_1)k_{l,s}^2 + a_1b_2 - a_2b_1$, the eigenvalues are given by

$$\lambda_{1,2}\left(k_{l,s}^2\right) = \frac{-p\left(k_{l,s}^2\right) \pm \sqrt{p^2\left(k_{l,s}^2\right) - 4q\left(k_{l,s}^2\right)}}{2}. \tag{32}$$

When the characteristic equation (31) has a characteristic root whose modulus is greater than 1, (30) is unstable. Therefore, according to the Jury criterion and Theorem 1, we obtain that the system (2) and (3) Turing instability condition is (10) holds and any one of the inequalities in condition (33) holds.

$$\begin{cases} 1 + p\left(k_{l,s}^2\right) + q\left(k_{l,s}^2\right) < 0, \\ 1 - p\left(k_{l,s}^2\right) + q\left(k_{l,s}^2\right) < 0, \\ q\left(k_{l,s}^2\right) > 1. \end{cases} \tag{33}$$

We can also analyze the stability of the system (30) in another, more direct way: the maximum value of $\|\lambda_{1,2}(k_{l,s}^2)\|$ is compared with 1.

Define

$$M = \max_{l,s=1}^{m}\left\{\max\left\{\left\|\lambda_1\left(k_{l,s}^2\right)\right\|, \left\|\lambda_2\left(k_{l,s}^2\right)\right\|\right\}\right\}, \tag{34}$$

$$\begin{aligned} &\theta_0, \theta_1 \in (0,\pi) \cup (\pi, 2\pi), \\ &D = \left\{(d_1, d_2) \,\middle|\, d_1 > 0, d_2 > 0\right\}, \\ &LS = \left\{(l,s) \,|\, l, s \in \mathbb{Z}^+, 1 \le l, s \le m\right\}, \\ &LS^* = \{(l,s) \mid (l,s) \in LS, (l,s) \ne (1,1)\}. \end{aligned} \tag{35}$$

To study the instability of the diffusion-driven, we choose (d_1, d_2) as the Turing bifurcation parameters, and then obtain the following theorem for the system (2) and (3).

Theorem 3. *For systems (2) and (3), we have*

(1) There exist a homogeneous stationary if $M < 1$

(2) The pure Turing instability occurs when the condition (10) and $M > 1$ are satisfied

(3) A Flip bifurcation occurs when the condition (10) holds and there exists $(l,s) \in LS$, $(d_1^*, d_2^*) \in D$ such that $1 - p(k_{l,s}^2) + q(k_{l,s}^2) = 0$, $|q(k_{l,s}^2)| < 1$, $M = |\lambda_1(k_{l,s})| = 1\,(\lambda_1(k_{l,s}) = -1, |\lambda_2(k_{l,s})| < 1)$ at $(d_1, d_2) = (d_1^*, d_2^*)$.

(4) A Neimark-Sacker bifurcation occurs when condition (10) holds and there exists $(l,s) \in LS$, $(d_1^*, d_2^*) \in D$ such that $|p(k_{l,s}^2)| < 2$, $q(k_{l,s}^2) = 1$, $M = \|\lambda_{1,2}(k_{l,s})\| = 1\,(\lambda_{1,2}(k_{l,s}) = e^{\pm i\theta_0})$ at $(d_1, d_2) = (d_1^*, d_2^*)$.

(5) A 1 : 2 Resonance occurs when the condition (10) holds and there exists $(l,s) \in LS$, $(d_1^*, d_2^*) \in D$ such that $1 - p(k_{l,s}^2) + q(k_{l,s}^2) = 0$, $q(k_{l,s}^2) = 1$, $M = |\lambda_{1,2}(k_{l,s})| = 1\,(\lambda_{1,2}(k_{l,s}) = -1)$ at $(d_1, d_2) = (d_1^*, d_2^*)$

(6) The pure Neimark-Sacker instability occurs when $\rho = \rho^*$, $|b(\rho^*)| < 2$, $c(\rho^*) = 1$, the transversality condition (12), $M = \|\lambda_{1,2}(k_{1,1})\| = 1\,(\lambda_{1,2}(k_{1,1}) = e^{\pm i\theta_0})$ are satisfied and $1 + p(k_{l,s}^2) + q(k_{l,s}^2) > 0$, $1 - p(k_{l,s}^2) + q(k_{l,s}^2) > 0$, $q(k_{l,s}^2) < 1$ hold for any $(l,s) \in LS^*$

(7) A Neimark-Sacker-Flip bifurcation occurs when $\rho = \rho^*$, $|b(\rho^*)| < 2$, $c(\rho^*) = 1$, the transversality condition (12) are satisfied and there exists $(l,s) \in LS^*$, $(d_1^*, d_2^*) \in D$ such that $1 - p(k_{l,s}^2) + q(k_{l,s}^2) = 0$, $|q(k_{l,s}^2)| < 1$, $M = \|\lambda_{1,2}(k_{1,1})\| = |\lambda_3(k_{l,s})| = 1\,(\lambda_{1,2}(k_{1,1}) = e^{\pm i\theta_0}, \lambda_3(k_{l,s}) = -1, |\lambda_4(k_{l,s})| < 1)$ at $(d_1, d_2) = (d_1^*, d_2^*)$

(8) A Neimark-Sacker-Neimark-Sacker bifurcation occurs when $\rho = \rho^*$, $|b(\rho^*)| < 2$, $c(\rho^*) = 1$, the transversality condition (12) are satisfied and there exists $(l,s) \in LS^*$, $(d_1^*, d_2^*) \in D$ such that $|p(k_{l,s}^2)| < 2$, $q(k_{l,s}^2) = 1$, $M = \|\lambda_{1,2}(k_{1,1})\| = \|\lambda_{3,4}(k_{l,s})\| = 1\,(\lambda_{1,2}(k_{1,1}) = e^{\pm i\theta_0}, \lambda_{3,4}(k_{l,s}) = e^{\pm i\theta_1})$ at $(d_1, d_2) = (d_1^*, d_2^*)$

(9) A Neimark-Sacker-Flip-Flip bifurcation occurs when $\rho = \rho^*$, $|b(\rho^*)| < 2$, $c(\rho^*) = 1$, the transversality condition (12) are satisfied and there exists $(l,s) \in LS^*$, $(d_1^*, d_2^*) \in D$ such that $1 - p(k_{l,s}^2) + q(k_{l,s}^2) = 0$, $q(k_{l,s}^2) = 1$, $M = \|\lambda_{1,2}(k_{1,1})\| = |\lambda_{3,4}(k_{l,s})| = 1\,(\lambda_{1,2}(k_{1,1}) = e^{\pm i\theta_0}, \lambda_{3,4}(k_{l,s}) = -1)$ at $(d_1, d_2) = (d_1^*, d_2^*)$

(10) The Neimark-Sacker-Turing instability occurs when $\rho = \rho^*$, $|b(\rho^*)| < 2$, $c(\rho^*) = 1$, the transversality condition (12) and $M > 1$ are satisfied

4. Application to a Modified Nicholson-Bailey Model

When $f(RH_n, P_n) = e^{-\gamma_1 T P_n}$, we obtain a classical Nicholson-Bailey model.

$$\begin{cases} H_{n+1} = RH_n e^{-\gamma_1 T P_n}, \\ P_{n+1} = kRH_n\left(1 - e^{-\gamma_1 T P_n}\right), \end{cases} \tag{36}$$

where $\gamma_1 > 0$ represents the rate at which parasitoids attack hosts and $T > 0$ is the duration of the host vulnerable stage [26, 27]. The dynamical properties of the Nicholson-Bailey model are well known. A host-parasitoid equilibrium is always present $(P^* = \ln(R)/\gamma_1 T > 0, H^* = \ln(R)/\gamma_1 T k(R-1) > 0)$ and this equilibrium is always locally unstable, with the slightest perturbation leading to oscillations of rapidly increasing amplitude [25], see Figure 2.

According to [22, 23], the parasitoid attack rate γ_1 decreases with increasing parasitoid density due to mutual interference of parasitoids, so Jervis and Murdoch redefine the parasitoid attack rate $\gamma_1 = \gamma_2 P_n^{-\sigma} > 0$, where the constant $\gamma_2 > 0$ and $0 \le \sigma < 1$ represent the mutual interference of parasitoids. For later analysis we write $\gamma = \gamma_2 T > 0$, such that $f(RH_n, P_n) = e^{-\gamma P_n^{1-\sigma}}$. Then, we obtain a modified Nicholson-Bailey model, rewriting the systems (1) and (2) as follows:

$$\begin{cases} H_{n+1} = RH_n e^{-\gamma P_n^{1-\sigma}}, \\ P_{n+1} = kRH_n\left(1 - e^{-\gamma P_n^{1-\sigma}}\right), \end{cases} \tag{37}$$

$$\begin{cases} H_{n+1}(i,j) = RH_n(i,j) e^{-\gamma P_n^{1-\sigma}(i,j)} + d_1 \nabla^2 H_n(i,j), \\ P_{n+1}(i,j) = kRH_n(i,j)\left(1 - e^{-\gamma P_n^{1-\sigma}(i,j)}\right) + d_2 \nabla^2 P_n(i,j). \end{cases} \tag{38}$$

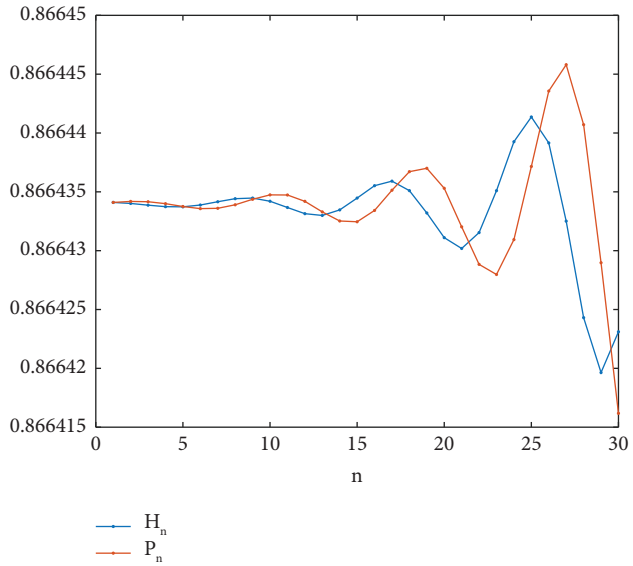

FIGURE 2: When $R = 2, k = 1, \gamma_1 = 0.8, T = 1$, the system (36) is unstable at the positive equilibrium point $(H^*, P^*) = (0.866434, 0.866434)$.

In the following, we perform theoretical analysis and numerical simulations of the systems (37) and (38) in conjunction with the theorems obtained in Section 3.

4.1. Stability Analysis of the Modified Nicholson-Bailey Model in the Absence of Diffusion. The positive equilibrium point of the system (37) can be obtained as $P^* = (\ln(R)/\gamma)^{1/1-\sigma} > 0, H^* = (\ln(R)/\gamma)^{1/1-\sigma}/k(R-1) > 0$, we have

$$RH^* \frac{\partial f(RH_n, P_n)}{\partial P_n}\bigg|_{H_n=H^*, P_n=P^*} = \frac{(-1+\sigma)\ln(R)}{k(R-1)},$$
$$RH^* \frac{\partial f(RH_n, P_n)}{\partial H_n}\bigg|_{H_n=H^*, P_n=P^*} = 0. \tag{39}$$

Putting (39) into (7), we get the following result:

$$a_1 = 1,$$
$$a_2 = \frac{(-1+\sigma)\ln(R)}{k(R-1)},$$
$$b_1 = k(R-1),$$
$$b_2 = \frac{(1-\sigma)\ln(R)}{(R-1)}. \tag{40}$$

According to (40) and (10), we have $b = -(a_1 + b_2) = -(1 + (1-\sigma)\ln(R)/R - 1)$, $c = a_1 b_2 - a_2 b_1 = (1-\sigma) R\ln(R)/R - 1$ and

$$\begin{cases} 1 + b + c = (1-\sigma)\ln(R) > 0, \\ 1 - b + c = 2 + \dfrac{(1-\sigma)(R+1)\ln(R)}{R-1} > 0, \\ 1 - c = 1 - \dfrac{(1-\sigma)R\ln(R)}{R-1}, \end{cases} \tag{41}$$

which means that the roots of the characteristic equation (8) will not equal 1 or -1 and when $R\ln(R) + 1 - R/R\ln(R) < \sigma < 1$, we have $1 - c = 1 - (1-\sigma)R\ln(R)/R - 1 > 0$. We know that $(x\ln(x) + 1 - x)|_{x=1} = 0$, and $d(x\ln(x) + 1 - x)/dx = \ln(x) > 0$ if $x > 1$, that means $R\ln(R) + 1 - R/R\ln(R) > 0$ because $R > 1$. According to Theorem 1, we can obtain the following corollary:

Corollary 1. *The system (37) is asymptotically stable at positive equilibrium (H^*, P^*) if and only if $R\ln(R) + 1 - R/R\ln(R) < \sigma < 1$.*

When $\sigma = 0$, the modified Nicholson-Bailey model (37) will degenerate to the classical Nicholson-Bailey model (36), which according to Corollary 1 does not satisfy the stability condition $R\ln(R) + 1 - R/R\ln(R) < \sigma < 1$. This is the reason why the classical Nicholson-Bailey model (36) is always unstable. Mutual interference of parasitoids σ is the key to the stability conditions that can exist in the modified Nicholson-Bailey model (37). Therefore, we choose σ as the Neimark-Sacker bifurcation parameter and then define $\sigma^* = R\ln(R) + 1 - R/R\ln(R)$, we have

$$\begin{cases} |b(\sigma^*)| = 1 + \dfrac{1}{R} < 2, \\ c(\sigma^*) = 1, \\ \dfrac{\partial c(\sigma)}{\partial \sigma}\bigg|_{\sigma=\sigma^*} = -\dfrac{R\ln(R)}{R-1} \neq 0. \end{cases} \tag{42}$$

According to Theorem 2, we can obtain the following corollary:

Corollary 2. *The system (37) undergoes a Neimark-Sacker bifurcation at $\sigma = \sigma^*$.*

4.2. Diffusion-Driven Instability Analysis of the Modified Nicholson-Bailey Model. According to (40), (31), and (33) we have

$$\begin{cases} p\left(k_{l,s}^2\right) = (d_1 + d_2)k_{l,s}^2 - \left(1 + \dfrac{(1-\sigma)\ln(R)}{R-1}\right), \\ q\left(k_{l,s}^2\right) = d_1 d_2 k_{l,s}^4 - \left(d_2 + \dfrac{d_1(1-\sigma)\ln(R)}{R-1}\right)k_{l,s}^2 + \dfrac{(1-\sigma)R\ln(R)}{R-1}, \end{cases} \tag{43}$$

$$\begin{cases} 1 + p\left(k_{l,s}^2\right) + q\left(k_{l,s}^2\right) = d_1 d_2 k_{l,s}^4 + d_1\left(1 - \dfrac{(1-\sigma)\ln(R)}{R-1}\right)k_{l,s}^2 + (1-\sigma)\ln(R), \\ 1 - p\left(k_{l,s}^2\right) + q\left(k_{l,s}^2\right) = d_1 d_2 k_{l,s}^4 - \left(d_1 + 2d_2 + \dfrac{d_1(1-\sigma)\ln(R)}{R-1}\right)k_{l,s}^2 + \left(2 + \dfrac{(R+1)(1-\sigma)\ln(R)}{R-1}\right), \\ 1 - q\left(k_{l,s}^2\right) = -d_1 d_2 k_{l,s}^4 + \left(d_2 + \dfrac{d_1(1-\sigma)\ln(R)}{R-1}\right)k_{l,s}^2 + 1 - \dfrac{(1-\sigma)R\ln(R)}{R-1}. \end{cases} \tag{44}$$

We know that $(x - 1 - \ln(x))|_{x=1} = 0$, and $d(x - 1 - \ln(x))/dx = 1 - 1/x > 0$ if $x > 1$, that means $0 < \ln(R)/R - 1 < 1$ because $R > 1$. There is always $(1 - (1 - \sigma)\ln(R)/R - 1) > 0$ such that $1 + p(k_{l,s}^2) + q(k_{l,s}^2) > 0$, which means that the positive real eigenvalues of the Jacobian matrix B do not cross the unit circle and Turing instability can only occur at $1 - p(k_{l,s}^2) + q(k_{l,s}^2) < 0$ or $q(k_{l,s}^2) > 1$.

According to Theorem 3 and Corollaries 1 and 2, we can obtain the following corollary:

Corollary 3. *For systems (38) and (3), we have*

(1) *There exist a homogeneous stationary if* $M < 1$

(2) *The pure Turing instability occurs when* $\sigma^* < \sigma < 1$ *and* $M > 1$ *are satisfied*

(3) *A Flip bifurcation occurs when* $\sigma^* < \sigma < 1$ *and there exists* $(l, s) \in LS$, $(d_1^*, d_2^*) \in D$ *such that* $1 - p(k_{l,s}^2) + q(k_{l,s}^2) = 0$, $|q(k_{l,s}^2)| < 1$, $M = |\lambda_1(k_{l,s})| = 1$ $(\lambda_1(k_{l,s}) = -1, |\lambda_2(k_{l,s})| < 1)$ *at* $(d_1, d_2) = (d_1^*, d_2^*)$

(4) *A Neimark-Sacker bifurcation occurs when* $\sigma^* < \sigma < 1$ *and there exists* $(l, s) \in LS$, $(d_1^*, d_2^*) \in D$ *such that* $|p(k_{l,s}^2)| < 2$, $q(k_{l,s}^2) = 1$, $M = \|\lambda_{1,2}(k_{l,s})\| = 1$ $(\lambda_{1,2}(k_{l,s}) = e^{\pm i\theta_0})$ *at* $(d_1, d_2) = (d_1^*, d_2^*)$

(5) *A 1 : 2 Resonance occurs when* $\sigma^* < \sigma < 1$ *and there exists* $(l, s) \in LS$, $(d_1^*, d_2^*) \in D$ *such that* $1 - p(k_{l,s}^2) + q(k_{l,s}^2) = 0$, $q(k_{l,s}^2) = 1$, $M = |\lambda_{1,2}(k_{l,s})| = 1$ $(\lambda_{1,2}(k_{l,s}) = -1)$ *at* $(d_1, d_2) = (d_1^*, d_2^*)$.

(6) *The pure Neimark-Sacker instability occurs when* $\sigma = \sigma^*$, $M = \|\lambda_{1,2}(k_{1,1})\| = 1$ $(\lambda_{1,2}(k_{1,1}) = e^{\pm i\theta_0})$ *are satisfied and* $1 - p(k_{l,s}^2) + q(k_{l,s}^2) > 0$, $q(k_{l,s}^2) < 1$ *hold for any* $(l, s) \in LS^*$

(7) *A Neimark-Sacker-Flip bifurcation occurs when* $\sigma = \sigma^*$ *and there exists* $(l, s) \in LS^*$, $(d_1^*, d_2^*) \in D$ *such that* $1 - p(k_{l,s}^2) + q(k_{l,s}^2) = 0$, $|q(k_{l,s}^2)| < 1$, $M = \|\lambda_{1,2}(k_{1,1})\| = |\lambda_3(k_{l,s})| = 1$ $(\lambda_{1,2}(k_{1,1}) = e^{\pm i\theta_0}$, $\lambda_3(k_{l,s}) = -1, |\lambda_4(k_{l,s})| < 1)$ *at* $(d_1, d_2) = (d_1^*, d_2^*)$

(8) *A Neimark-Sacker-Neimark-Sacker bifurcation occurs when* $\sigma = \sigma^*$ *and there exists* $(l, s) \in LS^*$, $(d_1^*, d_2^*) \in D$ *such that* $|p(k_{l,s}^2)| < 2$, $q(k_{l,s}^2) = 1$, $M = \|\lambda_{1,2}(k_{1,1})\| = \|\lambda_{3,4}(k_{l,s})\| = 1$ $(\lambda_{1,2}(k_{1,1}) = e^{\pm i\theta_0}$, $\lambda_{3,4}(k_{l,s}) = e^{\pm i\theta_1})$ *at* $(d_1, d_2) = (d_1^*, d_2^*)$

(9) *A Neimark-Sacker-Flip-Flip bifurcation occurs when* $\sigma = \sigma^*$ *and there exists* $(l, s) \in LS^*$, $(d_1^*, d_2^*) \in D$ *such that* $1 - p(k_{l,s}^2) + q(k_{l,s}^2) = 0$, $q(k_{l,s}^2) = 1$, $M = \|\lambda_{1,2}(k_{1,1})\| = |\lambda_{3,4}(k_{l,s})| = 1$ $(\lambda_{1,2}(k_{1,1}) = e^{\pm i\theta_0}$, $\lambda_{3,4}(k_{l,s}) = -1)$ *at* $(d_1, d_2) = (d_1^*, d_2^*)$.

(10) *The Neimark-Sacker-Turing instability occurs when* $\sigma = \sigma^*$ *and* $M > 1$ *are satisfied*

4.3. Numerical Simulation of the Modified Nicholson-Bailey Model

4.3.1. Numerical Simulation in the Absence of Diffusion. According to Corollaries 1 and 2, we have the following two sets of data:

(1) When $R = 2, k = 1, \gamma = 0.8, R\ln(R) + 1 - R/R\ln(R) = 0.278652$, we choose $\sigma = 0.5$ to satisfy Corollary 1, so system (37) is asymptotically stable at the positive equilibrium point $(H^*, P^*) = (0.750708, 0.750708)$ $(\lambda_{1,2} = 0.673287 \pm 0.489727\mathrm{i}, \|\lambda_{1,2}\| = 0.832554 < 1)$, parasite and host populations are maintained in a relatively stable state, see Figure 3

(2) When $R = 2, k = 1, \gamma = 0.8, \sigma^* = R\ln(R) + 1 - R/R\ln(R) = 0.278652$, we choose $\sigma = \sigma^*$ to satisfy Corollary 2, so near the positive equilibrium point, $(H^*P^*) = (0.819753, 0.819753)$, system (37) undergoes a Neimark-Sacker bifurcation at $\sigma = \sigma^*$ $(\lambda_{1,2} = 0.75 \pm 0.661438\mathrm{i}, \|\lambda_{1,2}\| = 1)$, parasite and host populations are maintained in a state of periodic oscillation, see Figure 4

We hope that the path to chaos can be found through a Neimark-Sacker bifurcation. Therefore, based on the second set of data, $R = 2, k = 1$ and $\gamma = 0.8$, we control the value of σ from 0.26 to 0.29 and draw diagram of the Neimark-Sacker bifurcation, see Figure 5 and the image of the maximum Lyapunov exponent about σ, see Figure 6. The maximum Lyapunov exponent is greater than 0, which means that chaos will occur in the system. Combining with

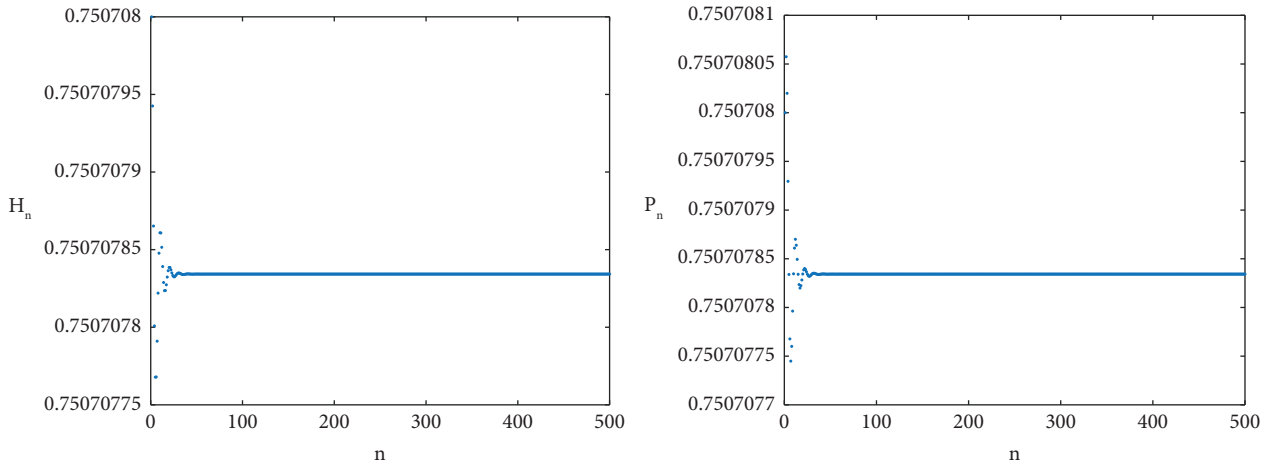

Figure 3: When $R = 2, k = 1, \gamma = 0.8, R\ln(R) + 1 - R/R\ln(R) = 0.278652, \sigma = 0.5$, system (37) is asymptotically stable at the positive equilibrium point $(H^*, P^*) = (0.750708, 0.750708)$. Parasite and host populations are maintained in a relatively stable state.

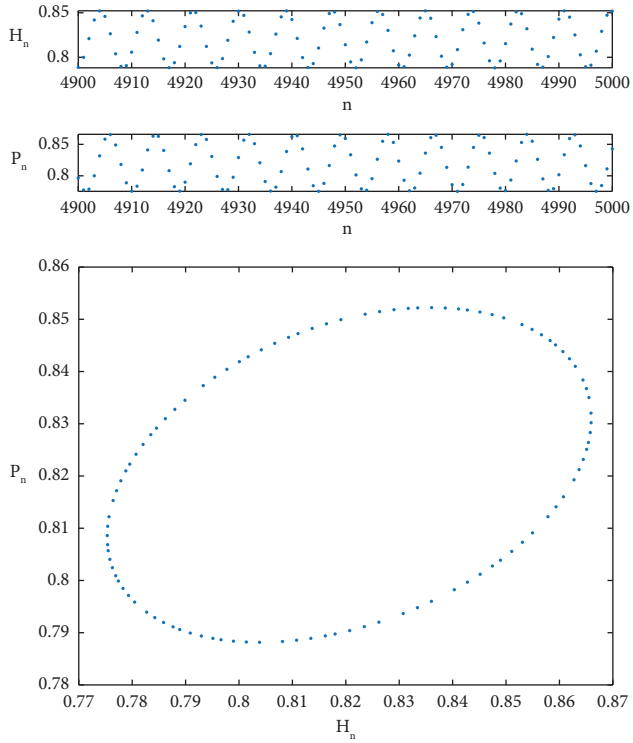

Figure 4: When $R = 2, k = 1, \gamma = 0.8, \sigma^* = 0.278652$, $(H^*, P^*) = (0.819753, 0.819753)$, system (37) undergoes a Neimark-Sacker bifurcation at $\sigma = \sigma^*$. Parasite and host populations are maintained in a state of periodic oscillation.

Figures 4–6, we can clearly see that when $\sigma > \sigma^*$, system (37) remains in a stable state, and the maximum Lyapunov exponent is less than 0. When $\sigma = \sigma^*$, system (37) undergoes a Neimark-Sacker bifurcation, and the maximum Lyapunov exponent is equal to 0. When $\sigma < \sigma^*$, the original periodic oscillation of system (37) is gradually broken, chaos occurs, and the maximum Lyapunov exponent is greater than 0.

4.3.2. Numerical Simulation of Diffusion-Driven Instability. This part mainly combines the content of Corollary 3 to carry out numerical simulation of systems (38) and (3). It is important to note here that the size of the region we simulate numerically is $(m + 2) \times (m + 2)$ and where m is equal to 64. Since $H_n(i, j)$ and $H_n(i, j)$ cannot be negative, the following definition is to be made:

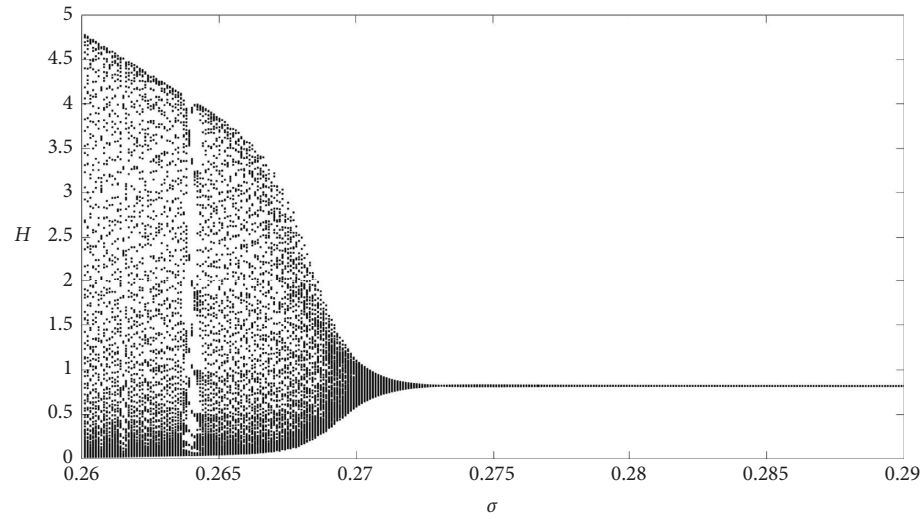

FIGURE 5: The diagram of the Neimark-Sacker bifurcation, where $R = 2, k = 1, \gamma = 0.8, \sigma^* = 0.278652$ and the value of σ from 0.26 to 0.29.

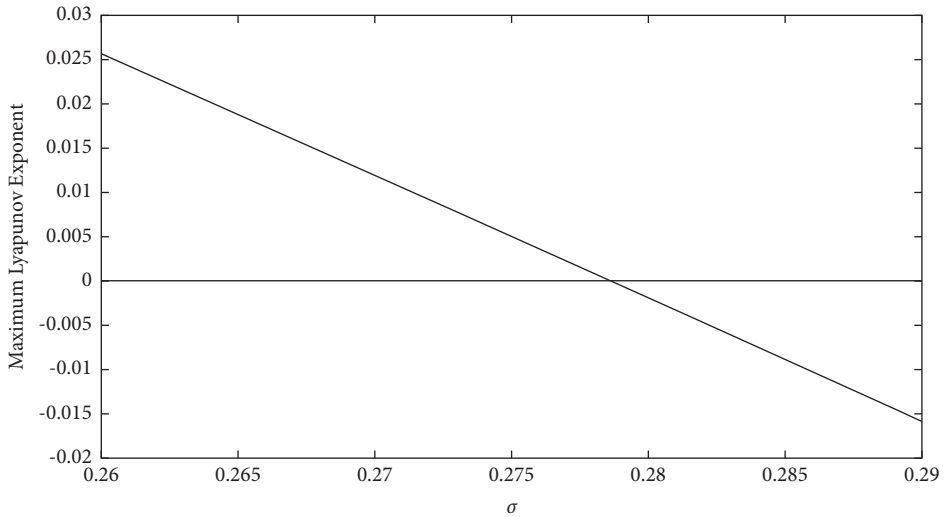

FIGURE 6: The image of the maximum Lyapunov exponent about σ, where $R = 2, k = 1, \gamma = 0.8, \sigma^* = 0.278652$ and the value of σ from 0.26 to 0.29.

$$\begin{aligned} &\text{if } H_n(i,j) < 0, \text{let } H_n(i,j) = 0, \\ &\text{if } P_n(i,j) < 0, \text{let } P_n(i,j) = 0, \end{aligned} \tag{45}$$

where $1 \le i, j \le 64$ and $i, j, n \in \mathbb{Z}^+$. We take a random matrix approach to assign initial values to internal points, and then combine the boundary conditions to assign initial values to boundary points as follows:

$$\begin{aligned} HH &= \text{rand}(64), \\ PP &= \text{rand}(64), \\ H_0(i,j) &= H^* + 0.00000001HH(i,j), \\ P_0(i,j) &= P^* + 0.00000001PP(i,j), \end{aligned} \tag{46}$$

where $i, j \in \mathbb{Z}^+, 1 \le i, j \le 64$, rand(64) stands for randomly generating a square matrix of order 64, where the maximum and minimum values of the elements are 1 and 0, respectively. Then, the boundary points are assigned initial values according to the periodic boundary condition (3) as follows:

$$\begin{aligned} H_0(i,0) &= H_0(i,64), H_0(0,j) = H_0(64,j), \\ H_0(i,65) &= H_0(i,1), H_0(65,j) = H_0(1,j), \\ P_0(i,0) &= P_0(i,64), P_0(0,j) = P_0(64,j), \\ P_0(i,65) &= P_0(i,1), P_0(65,j) = P_0(1,j), \end{aligned} \tag{47}$$

where $1 \le i, j \le 64, i, j, \in \mathbb{Z}^+$.

By numerical simulation, we obtain some parameter planes of M as follows:

(1) The parameter planes of M with respect to d_1 and σ, see Figure 7

(2) The parameter planes of M with respect to d_2 and σ, see Figure 8

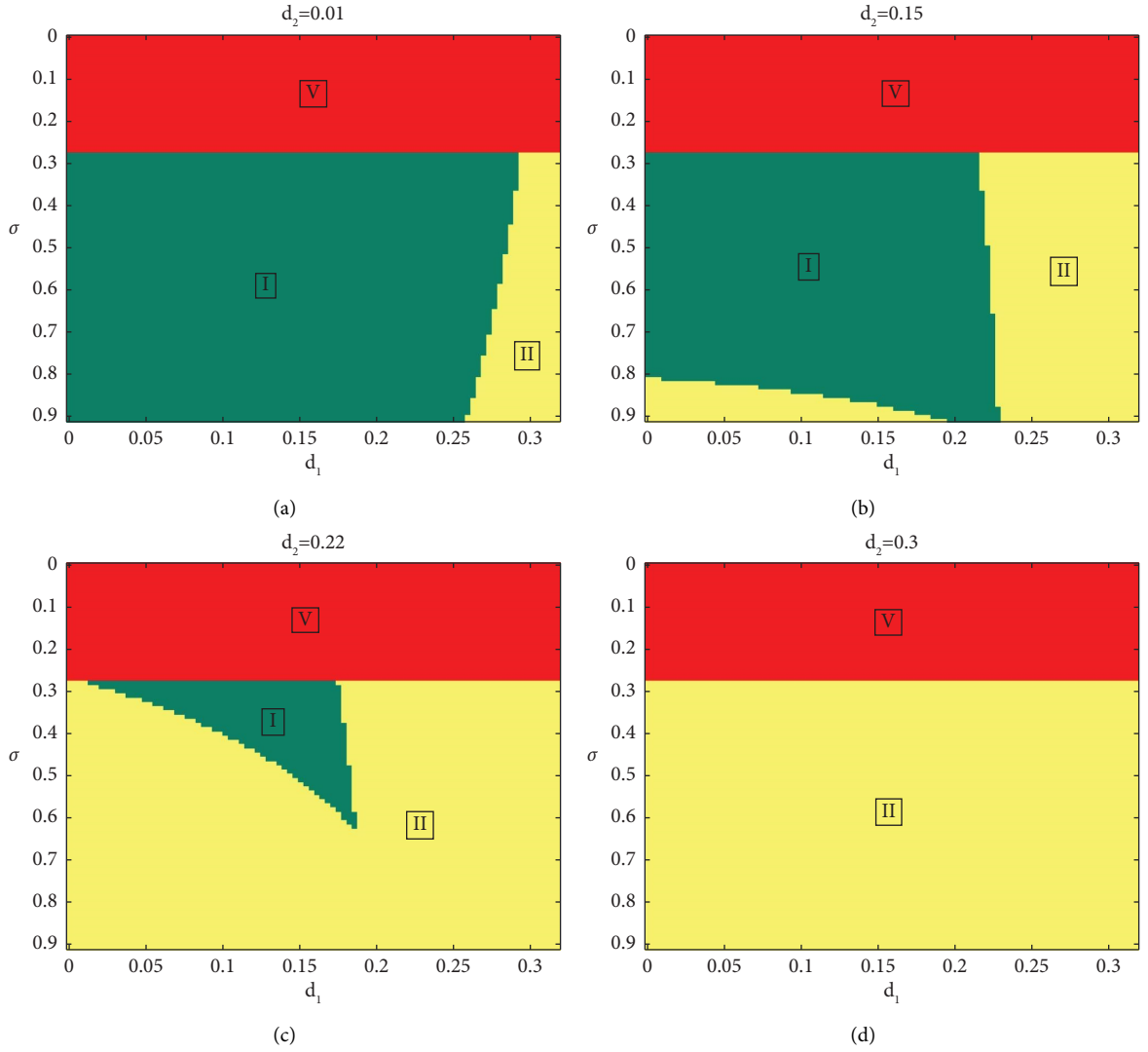

Figure 7: (*a*), (*b*), (*c*), (*d*) are parameter planes of M with respect to d_1 and σ, we choose $R = 2, k = 1, \gamma = 0.8, \sigma^* = 0.278655$, and $d_2 = 0.01$ in (a), $d_2 = 0.15$ in (b), $d_2 = 0.22$ in (c), $d_2 = 0.3$ in (d). The results show that $M < 1$ in region I and $M > 1$ in regions II and V.

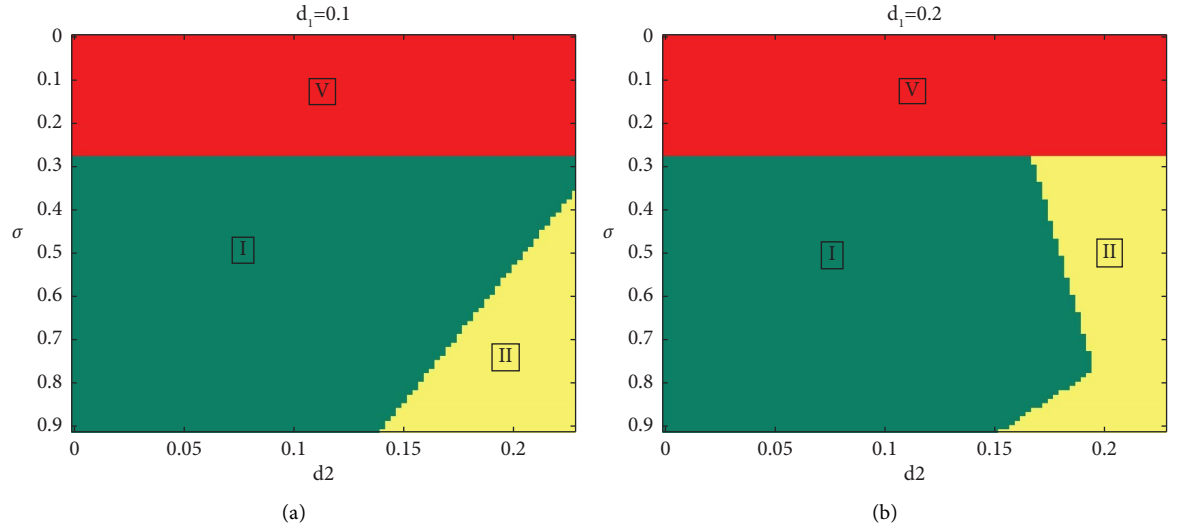

Figure 8: Continued.

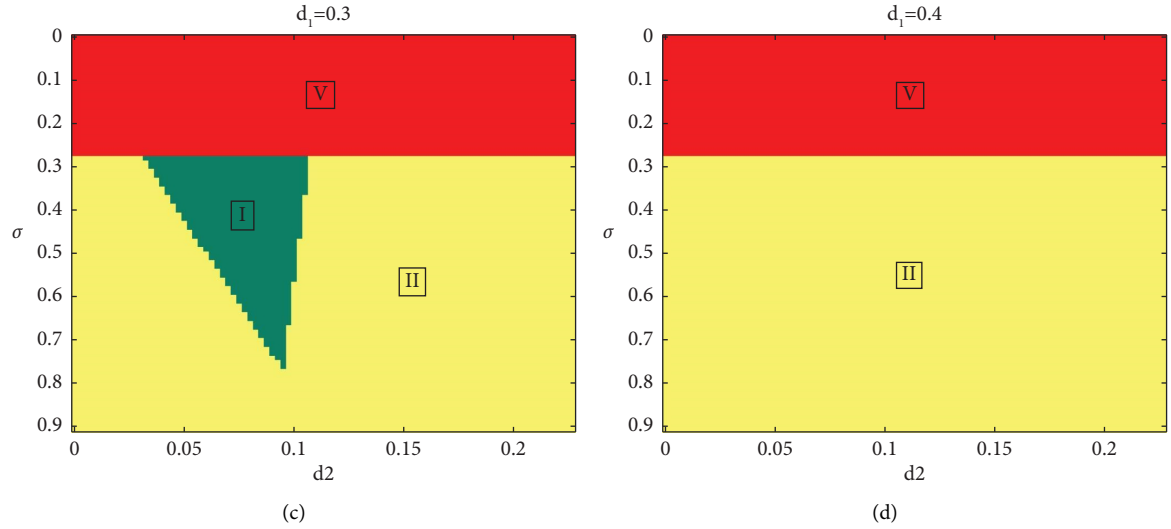

FIGURE 8: (*a*), (*b*), (*c*), (*d*) are parameter planes of M with respect to d_2 and σ, we choose $R = 2, k = 1, \gamma = 0.8, \sigma^* = 0.278655$, and $d_1 = 0.1$ in (a), $d_1 = 0.2$ in (b), $d_1 = 0.3$ in (c), $d_1 = 0.4$ in (d). The results show that $M < 1$ in region I and $M > 1$ in regions II and V.

(3) The parameter planes of M with respect to d_1 and d_2, see Figure 9

To summarize, regions I–V in Figures 7–9 represent the following meanings:

(1) Region I represents $\sigma_* < \sigma < 1$ and $M < 1$ (a homogeneous stationary occurs)

(2) Region II represents $\sigma_* < \sigma < 1$ and $M > 1$ (the pure Turing instability occurs)

(3) Region III represents $\sigma = \sigma_*$ and $M = 1$ (the pure Neimark-Sacker instability occurs)

(4) Region IV represents $\sigma = \sigma_*$ and $M > 1$ (the Neimark-Sacker-Turing instability occurs)

(5) Region V represents $0 < \sigma < \sigma_*$ and $M > 1$ (the instability occurs)

According to Corollary 3, we have the following numerical simulation results for systems (38) and (3):

(1) We choose $d_1 = 0.2, \sigma^* < \sigma = 0.75 < 1$, and the other parameters are consistent with Figure 7, then we have

(a) When $d_2 = 0.15$, (d_1, σ) will fall in the region I of Figure 7(b), which is consistent with the case of Corollary 3(1), there exist a homogeneous stationary, parasite and host populations are maintained in a relatively stable state in two-dimensional space, see Figure 10

(b) When $d_2 = 0.22$, (d_1, σ) will fall in the region II of Figure 7(c), which is consistent with the case of Corollary 3(2), the pure Turing instability occurs, parasite and host populations exhibit an extremely unstable state in two-dimensional space, see Figure 11

(2) We choose $d_2 = 0.175, \sigma^* < \sigma = 0.75 < 1$, and the other parameters are consistent with Figure 8, then we have

(a) When $d_1 = 0.1$, (d_2, σ) will fall in the region II of Figure 8(a), which is consistent with the case of Corollary 3(2), the pure Turing instability occurs, parasite and host populations exhibit an extremely unstable state in two-dimensional space, see Figure 12

(b) When $d_1 = 0.2$, (d_2, σ) will fall in the region I of Figure 8(b), which is consistent with the case of Corollary 3(1), there exist a homogeneous stationary, parasite and host populations are maintained in a relatively stable state in two-dimensional space, see Figure 13

(3) We choose $\sigma^* < \sigma = 0.5 < 1$, and the other parameters are consistent with Figure 9, then we have the following results:

(a) When $d_1 = 0.15$ and $d_2 = 0.222474$, (d_1, d_2) will fall at the junction of regions I and II in Figure 9(a), and there exists $(l, s) = (33, 33) \in LS$ such that $1 - p(k_{l,s}^2) + q(k_{l,s}^2) = 0$, $|q(k_{l,s}^2)| = 0.633215 < 1$, $M = |\lambda_1(k_{l,s})| = 1$ ($\lambda_1(k_{l,s}) = -1, |\lambda_2(k_{l,s})| = 0.633215 < 1$). According to Corollary 3(3), a Flip bifurcation occurs, parasite and host populations exhibit period-doubling in two-dimensional space, see Figures 14 and 15

(b) When $d_1 = 0.2$ and $d_2 = 0.179452$, (d_1, d_2) will fall at the junction of regions I and II in Figure 9(a), and there exists $(l, s) = (33, 33) \in LS$ such that $|p(k_{l,s}^2)| = 1.689042 < 2$, $q(k_{l,s}^2) = 1$, $M = \|\lambda_{1,2}(k_{l,s})\| = 1$ ($\lambda_{1,2}(k_{l,s}) = -0.844521 \pm 0.535521\mathrm{i}$). According to Corollary 3(4),

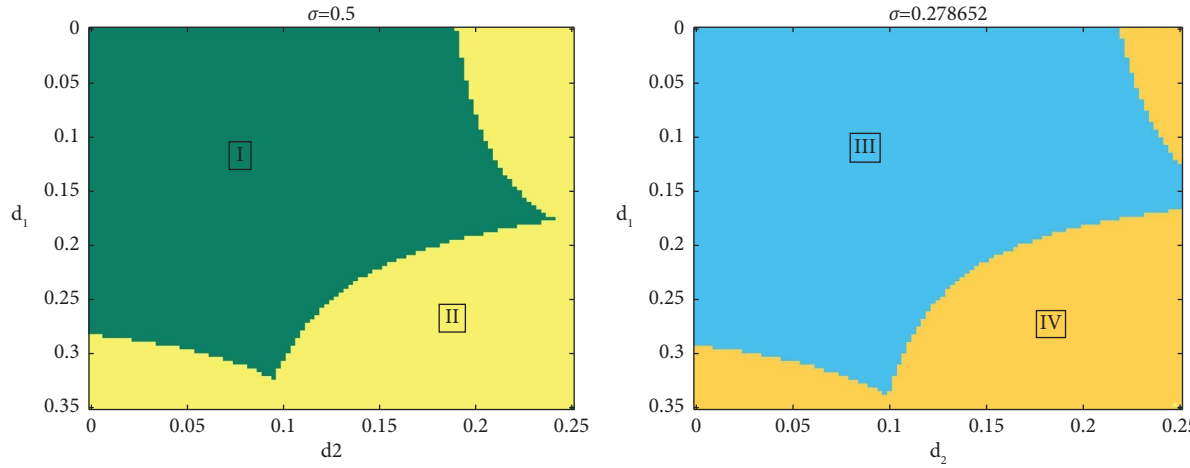

Figure 9: (*a*), (*b*) are parameter planes of M with respect to d_1 and d_2, we choose $R = 2, k = 1, \gamma = 0.8, \sigma^* = 0.278655$, and $\sigma^* < \sigma = 0.5 < 1$ in (a), $\sigma = \sigma^*$ in (b). The results show that $M < 1$ in region I $M = 1$ in region III, and $M > 1$ in regions II, IV.

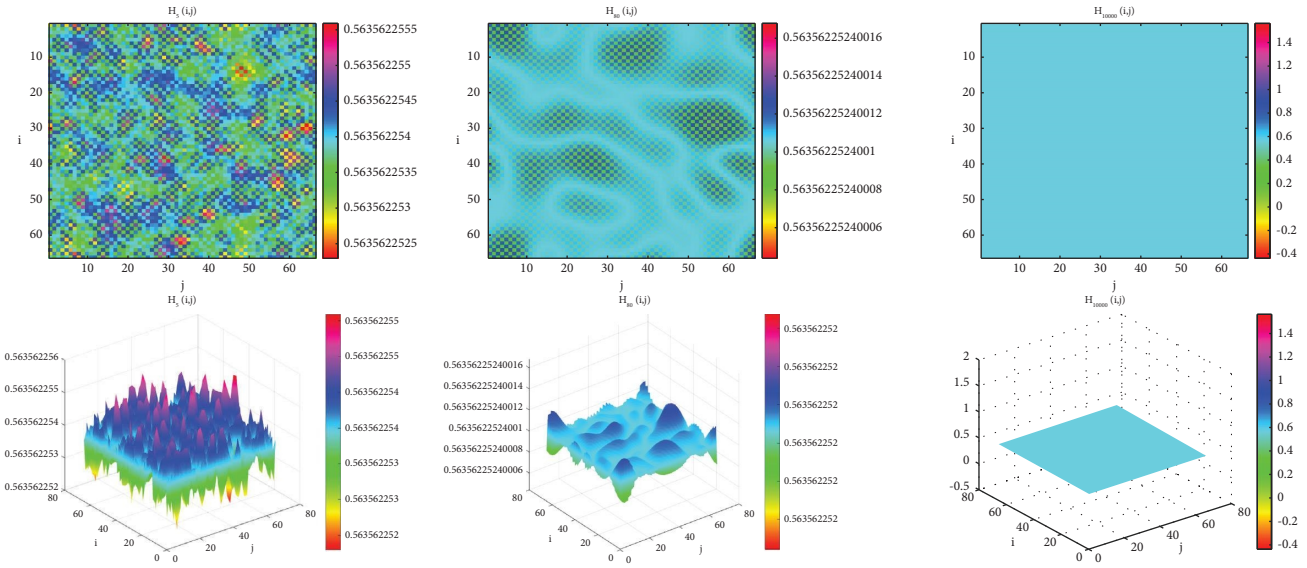

Figure 10: Continued.

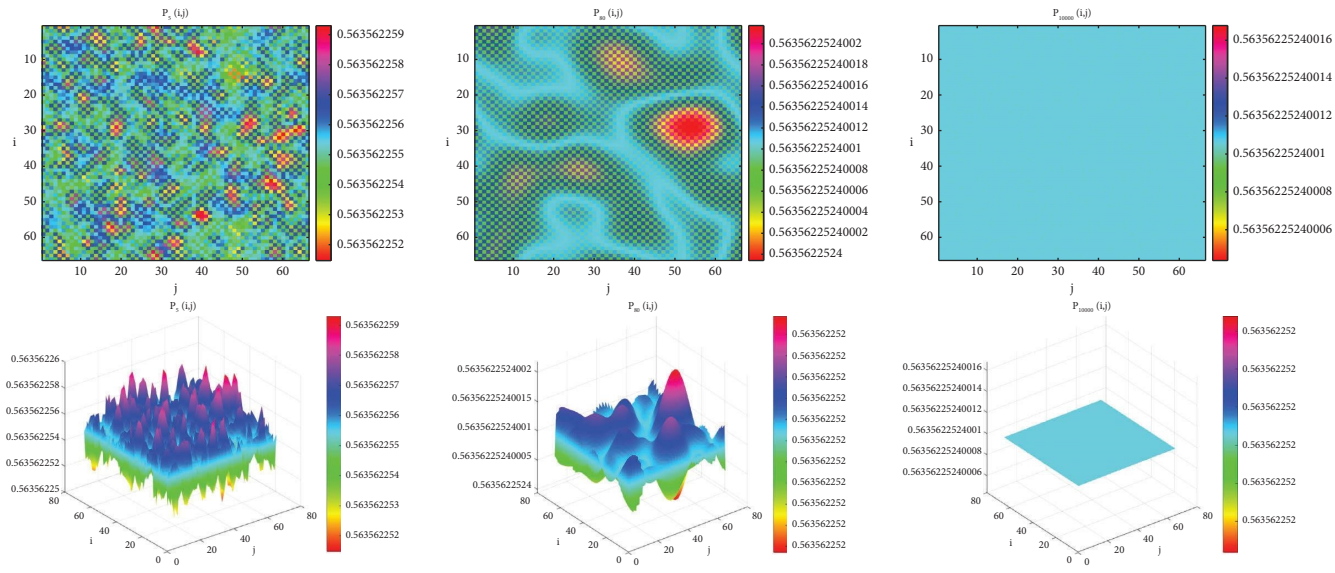

(d) (e) (f)

FIGURE 10: $R = 2, k = 1, \gamma = 0.8, \sigma^* = 0.278655, d_2 = 0.15, (d_1, \sigma) = (0.2, 0.75)$ falls in the region I of Figure 7(b), which is consistent with the case of Corollary 3(1), there exist a homogeneous stationary, parasite and host populations are maintained in a relatively stable state in two-dimensional space.

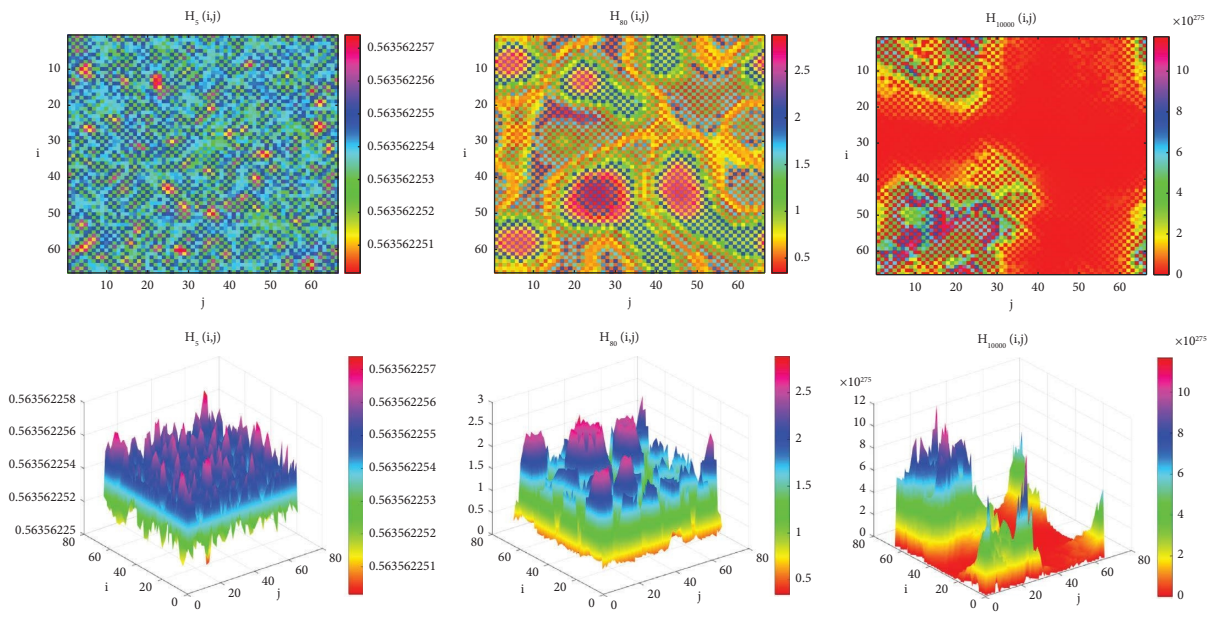

(a) (b) (c)

FIGURE 11: Continued.

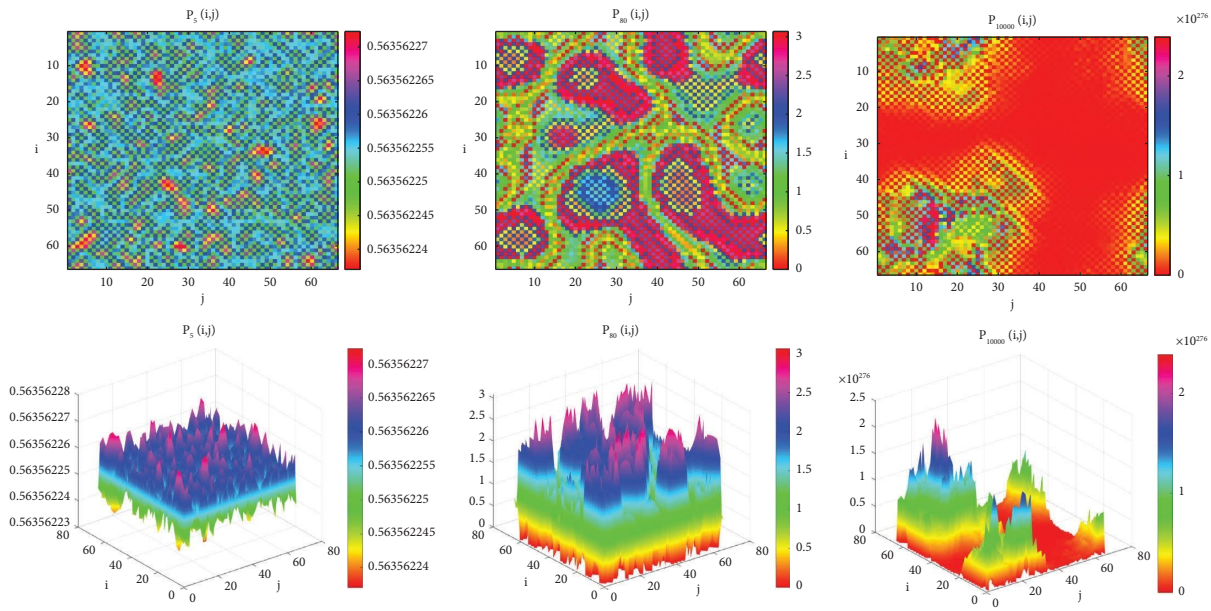

Figure 11: $R = 2, k = 1, \gamma = 0.8, \sigma^* = 0.278655, d_2 = 0.22, (d_1, \sigma) = (0.2, 0.75)$ falls in the region II of Figure 7(c), which is consistent with the case of Corollary 3(2), the pure Turing instability occurs, parasite and host populations are maintained in a relatively stable state in two-dimensional space.

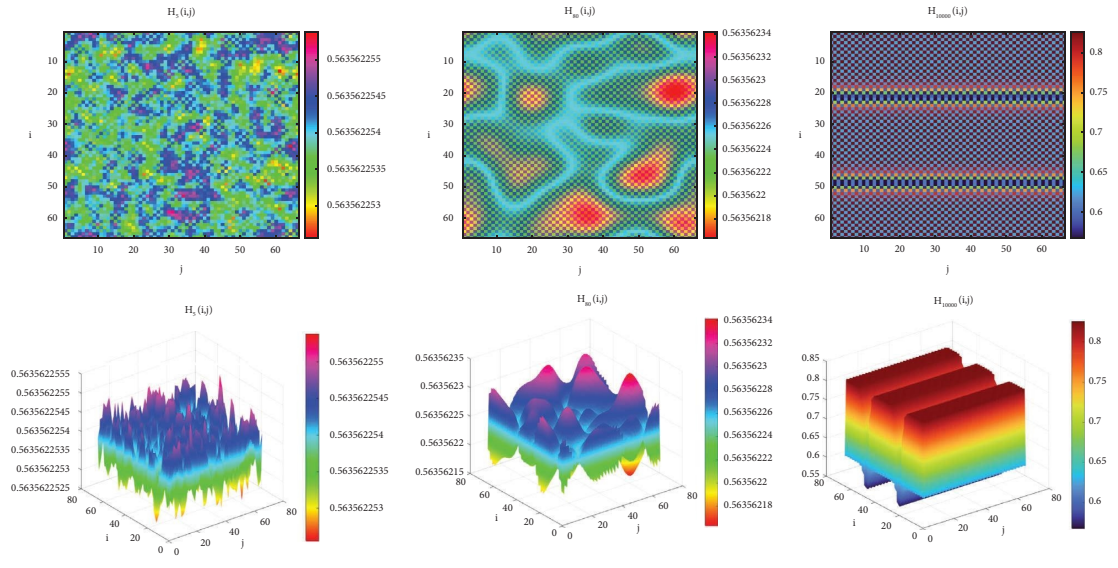

Figure 12: Continued.

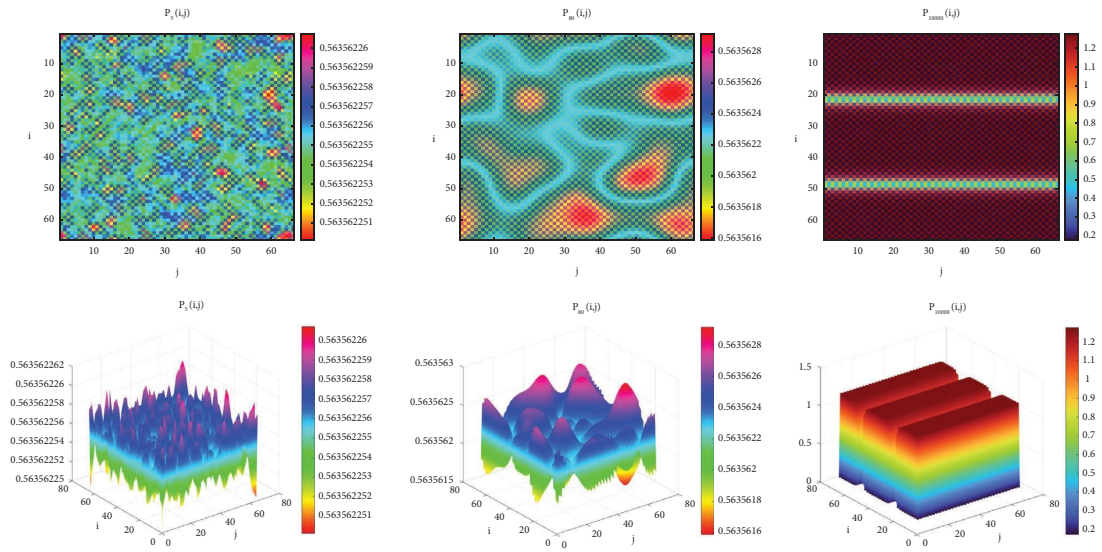

(d) (e) (f)

FIGURE 12: $R = 2, k = 1, \gamma = 0.8, \sigma^* = 0.278655, d_1 = 0.1, (d_2, \sigma) = (0.175, 0.75)$ falls in the region II of Figure 8(a), which is consistent with the case of Corollary 3(2), the pure Turing instability occurs, parasite and host populations exhibit an extremely unstable state in two-dimensional space.

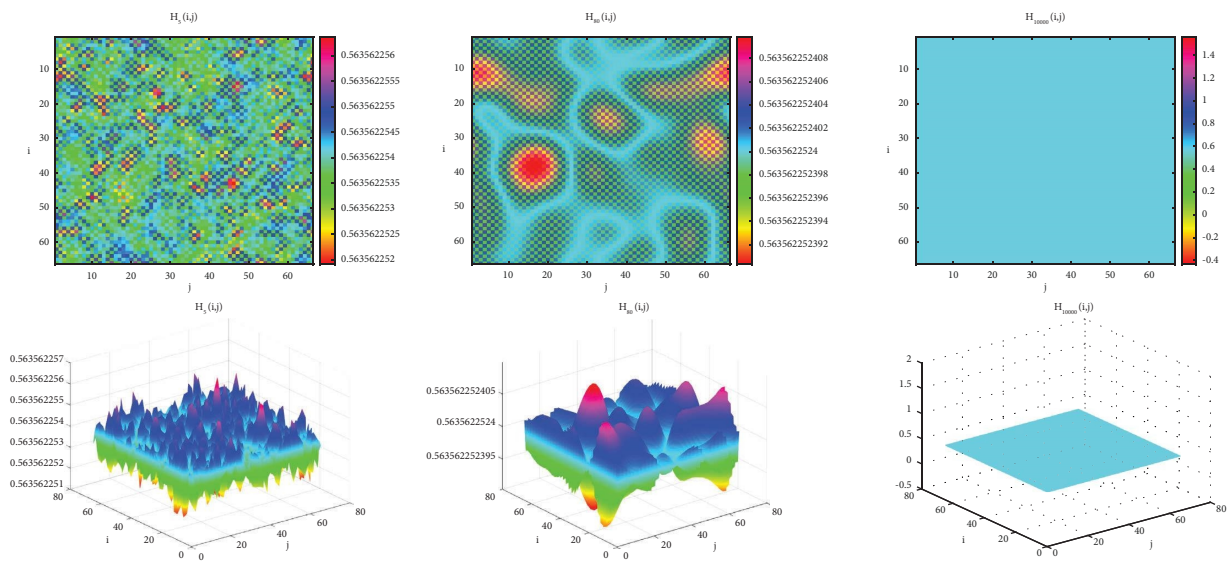

(a) (b) (c)

FIGURE 13: Continued.

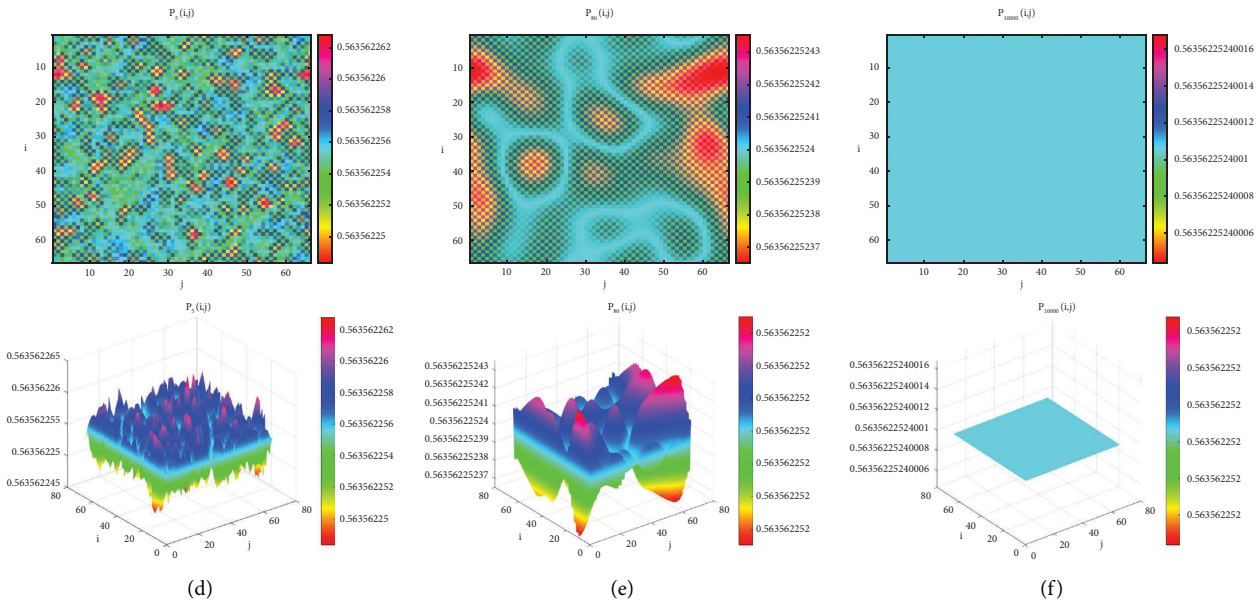

(d) (e) (f)

FIGURE 13: $R = 2, k = 1, \gamma = 0.8, \sigma^* = 0.278655, d_1 = 0.2, (d_2, \sigma) = (0.175, 0.75)$ falls in the region I of Figure 8(b), which is consistent with the case of Corollary 3(1), there exist a homogeneous stationary, parasite and host populations are maintained in a relatively stable state in two-dimensional space.

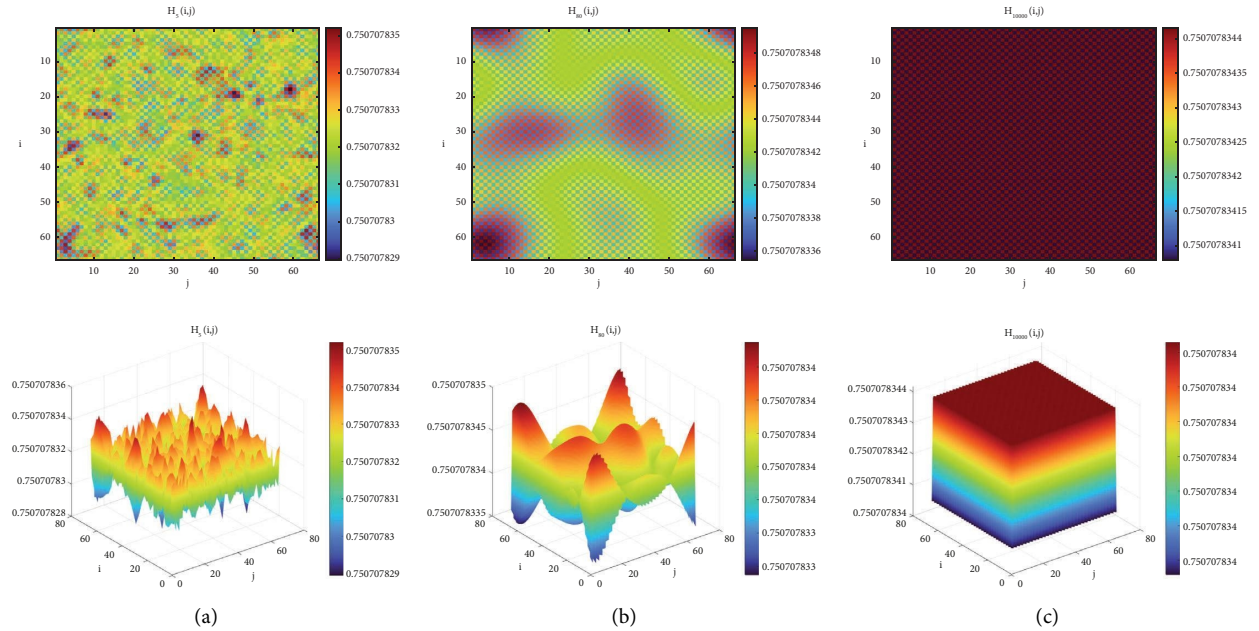

(a) (b) (c)

FIGURE 14: Continued.

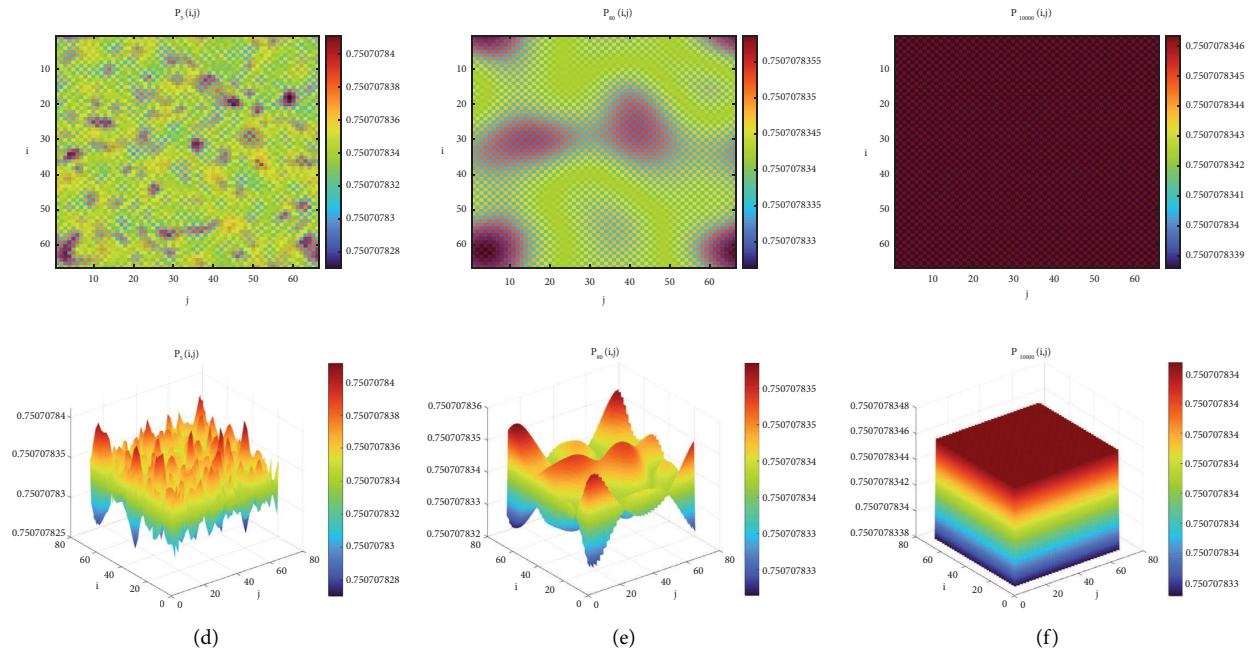

(d) (e) (f)

Figure 14: $R = 2, k = 1, \gamma = 0.8, \sigma^* = 0.278655, \sigma = 0.5, (d_1, d_2) = (0.15, 0.222474)$ falls at the junction of regions I and II in Figure 9(a), which is consistent with the case of Corollary 3(3), a Flip bifurcation occurs, parasite and host populations exhibit period-doubling in two-dimensional space.

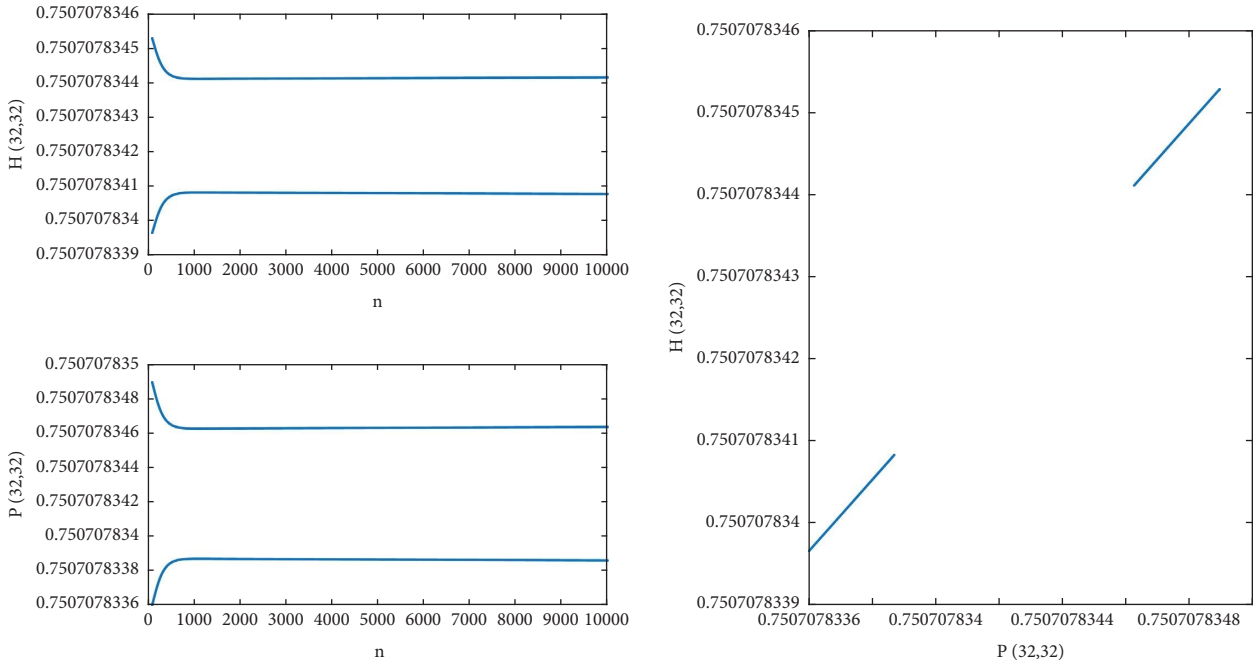

Figure 15: $R = 2, k = 1, \gamma = 0.8, \sigma^* = 0.278655, \sigma = 0.5, (d_1, d_2) = (0.15, 0.222474)$ falls at the junction of regions I and II in Figure 9(a), which is consistent with the case of Corollary 3(3), a Flip bifurcation occurs, parasite and host populations exhibit period-doubling.

a Neimark-Sacker bifurcation occurs, parasite and host populations exhibit periodic oscillations in two-dimensional space, see Figures 16 and 17.

(c) When $d_1 = 0.176412$ and $d_2 = 0.24191$, (d_1, d_2) will fall at the junction of regions I and II in Figure 9(a), and there exists $(l, s) = (33, 33) \in LS$ such that $1 - p(k_{l,s}^2) + q(k_{l,s}^2) = 0$, $q(k_{l,s}^2) = 1$,

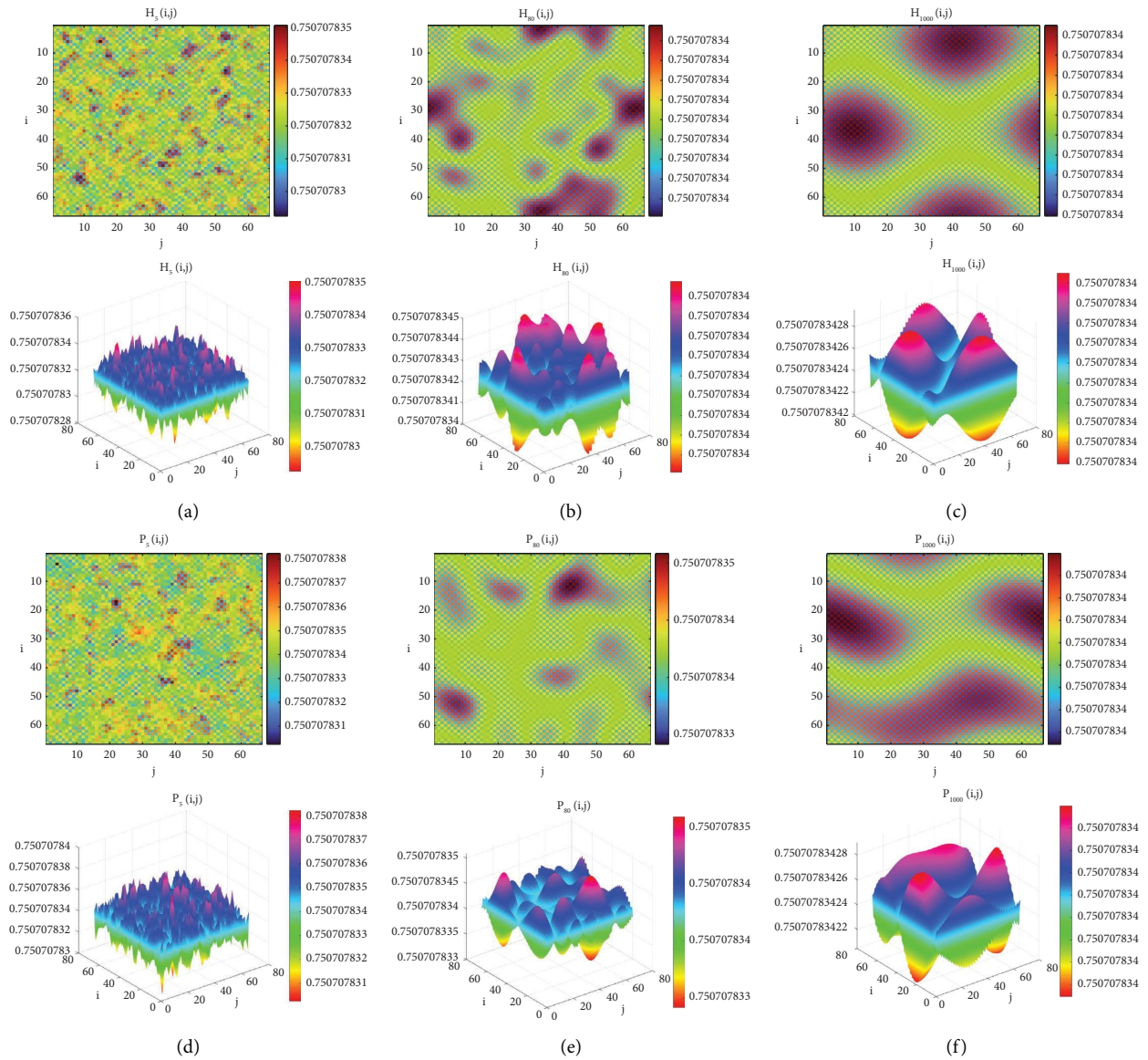

FIGURE 16: $R = 2, k = 1, \gamma = 0.8, \sigma^* = 0.278655, \sigma = 0.5, (d_1, d_2) = (0.2, 0.179452)$ falls at the junction of regions I and II in Figure 9(a), which is consistent with the case of Corollary 3(4), a Neimark-Sacker bifurcation occurs, parasite and host populations exhibit periodic oscillations in two-dimensional space.

$M = |\lambda_{1,2}(k_{l,s})| = 1$ $(\lambda_{1,2}(k_{l,s}) = -1)$. According to Corollary 3(5), a 1 : 2 Resonance occurs, parasite and host populations exhibit unstable period-doubling oscillations in two-dimensional space, see Figures 18 and 19.

(4) We choose $\sigma = \sigma^* = 0.278652$ $(\lambda_{1,2}(k_{1,1}) = 0.75 \pm 0.661438\mathrm{i})$, and the other parameters are consistent with Figure 9, then we have the following results:

(a) When $d_1 = 0.1$ and $d_2 = 0.1$, (d_1, d_2) will fall in the region III of Figure 9(b), and $1 - p(k_{l,s}^2) + q(k_{l,s}^2) > 0$, $q(k_{l,s}^2) < 1$, $M = \|\lambda_{1,2}(k_{1,1})\| = 1$ hold for any $(l, s) \in LS^*$. According to Corollary 3(6), the pure Neimark-Sacker instability occurs, parasite and host populations exhibit periodic oscillatory behavior in two-dimensional space, see Figures 20 and 21.

(b) When $d_1 = 0.3$ and $d_2 = 0.03125$, (d_1, d_2) will fall at the junction of regions III and IV in Figure 9(b), and there exists $(l, s) = (33, 33) \in LS^*$ such that $1 - p(k_{l,s}^2) + q(k_{l,s}^2) = 0$, $|q(k_{l,s}^2)| = 0.15 < 1$, $M = \|\lambda_{1,2}(k_{1,1})\| = |\lambda_3(k_{l,s})| = 1$ $(\lambda_3(k_{l,s}) = -1, |\lambda_4(k_{l,s})| = 0.15 < 1)$. According to Corollary 3(7), a Neimark-Sacker-Flip bifurcation occurs, the number of parasites and hosts in two-dimensional space can show periodic doubling and periodic oscillation alternately, see Figures 22 and 23.

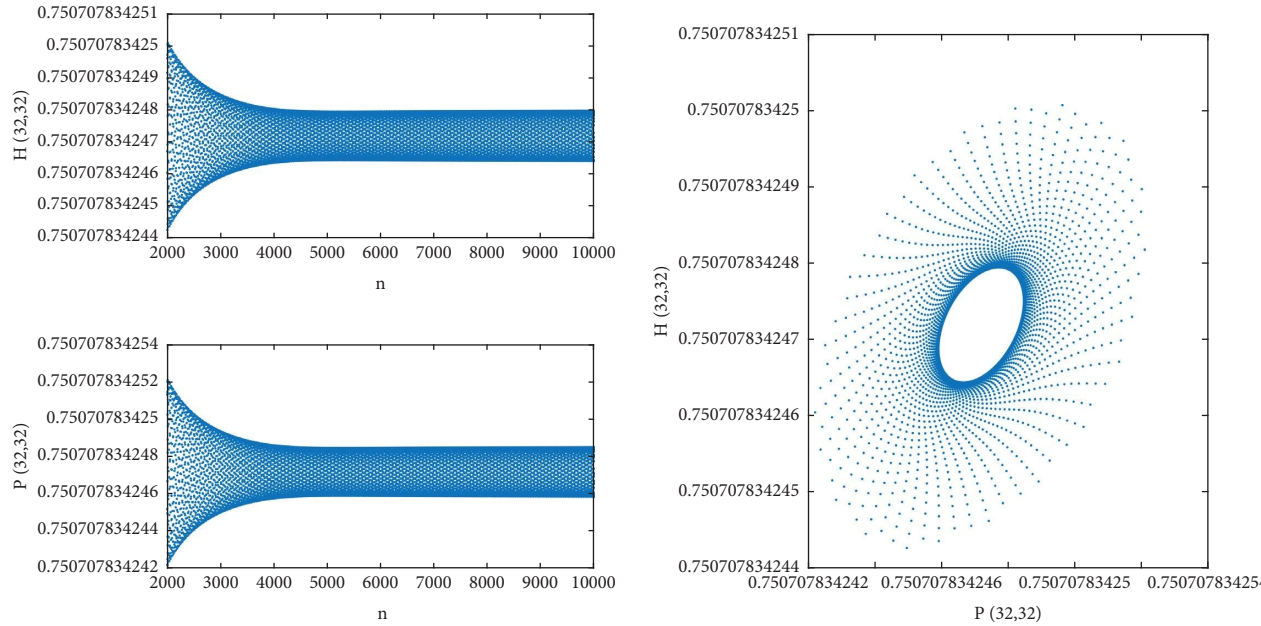

Figure 17: $R = 2, k = 1, \gamma = 0.8, \sigma^* = 0.278655, \sigma = 0.5, (d_1, d_2) = (0.2, 0.179452)$ falls at the junction of regions I and II in Figure 9(a), which is consistent with the case of Corollary 3(4), a Neimark-Sacker bifurcation occurs, parasite and host populations exhibit periodic oscillations.

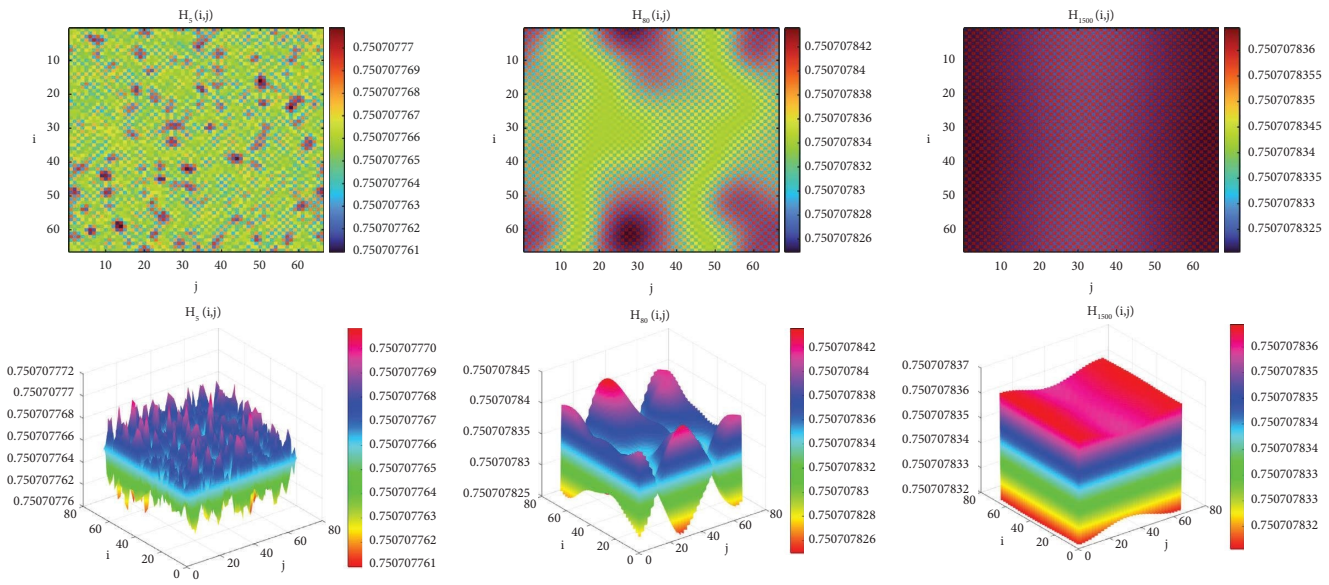

Figure 18: Continued.

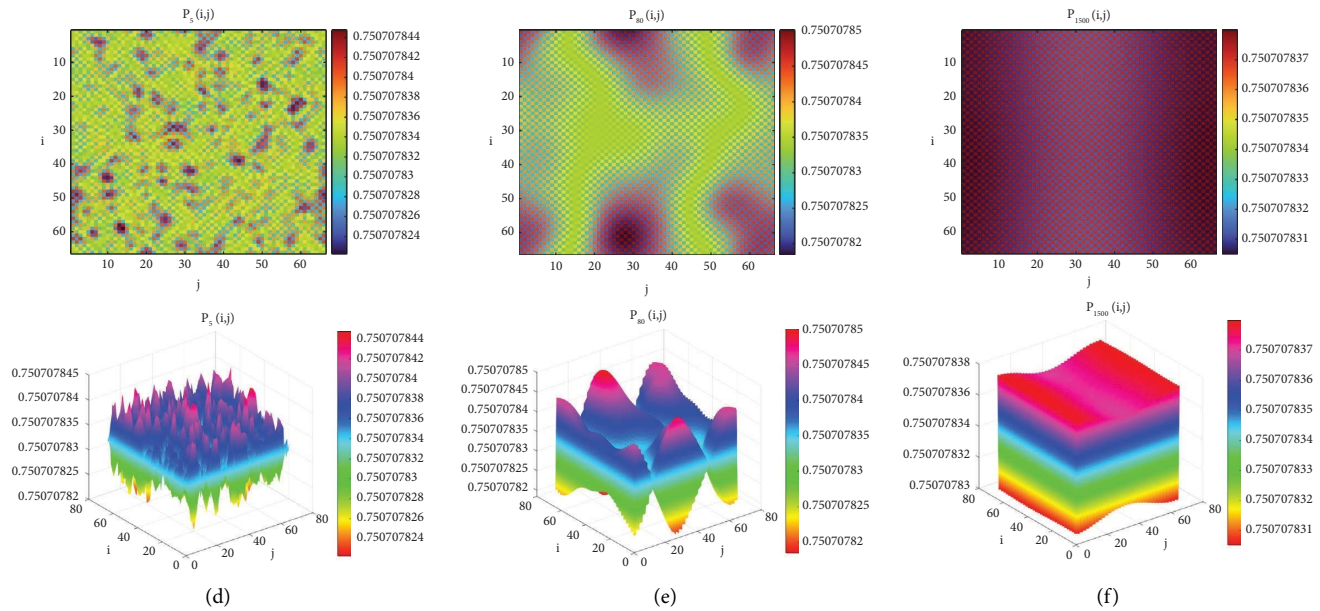

FIGURE 18: $R = 2, k = 1, \gamma = 0.8, \sigma^* = 0.278655, \sigma = 0.5, (d_1, d_2) = (0.176412, 0.24191)$ falls at the junction of regions I and II in Figure 9(a), which is consistent with the case of Corollary 3(5), a 1 : 2 Resonance occurs, parasite and host populations exhibit unstable period-doubling oscillations in two-dimensional space.

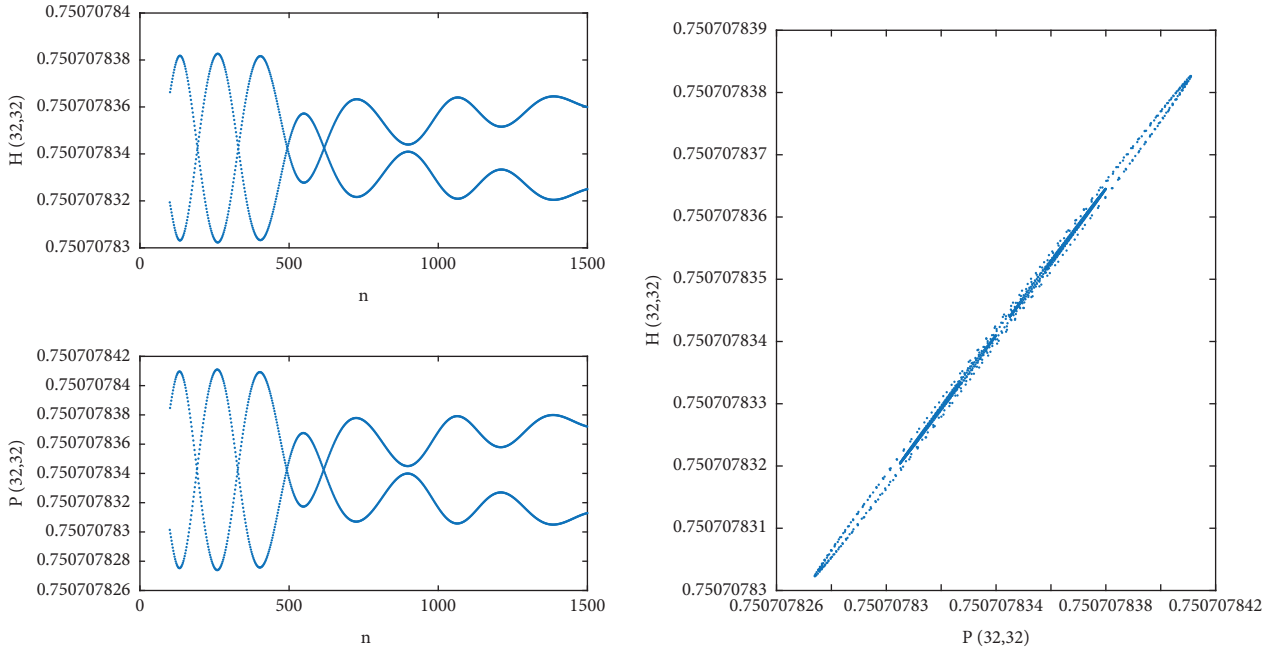

FIGURE 19: $R = 2, k = 1, \gamma = 0.8, \sigma^* = 0.278655, \sigma = 0.5, (d_1, d_2) = (0.176412, 0.24191)$ falls at the junction of regions I and II in Figure 9(a), which is consistent with the case of Corollary 3(5), a 1 : 2 Resonance occurs, parasite and host populations exhibit unstable period-doubling oscillations.

(c) When $d_1 = 0.2$ and $d_2 = 0.166667$, (d_1, d_2) will fall at the junction of regions III and IV in Figure 9(b), and there exists $(l, s) = (33, 33) \in LS^*$ such that $|p(k_{l,s}^2)| = 1.433336 < 2$, $q(k_{l,s}^2) = 1$, $M = \|\lambda_{1,2}(k_{1,1})\| = \|\lambda_{3,4}(k_{l,s})\| = 1$ $(\lambda_{3,4}(k_{l,s}) = -0.716668 \pm 0.697416i)$. According to Corollary 3(8), a Neimark-Sacker-Neimark-Sacker bifurcation occurs, parasite and host populations generally exhibit periodic oscillatory behavior in two-dimensional space, see Figures 24 and 25.

(d) When $d_1 = 0.161612$ and $d_2 = 0.275888$, (d_1, d_2) will fall at the junction of regions III and IV in Figure 9(b), and there exists $(l, s) = (33, 33) \in$

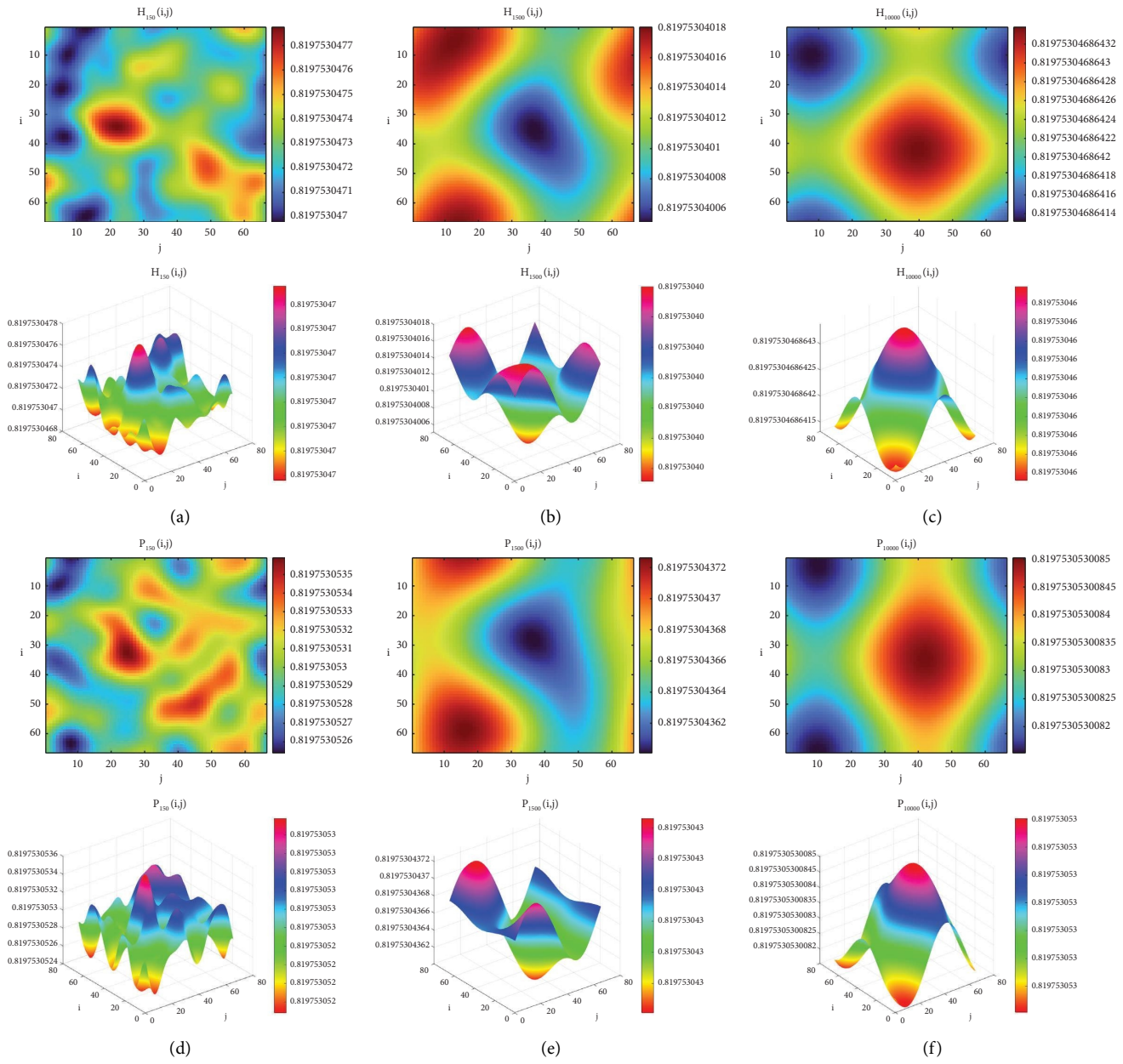

FIGURE 20: $R = 2, k = 1, \gamma = 0.8, \sigma^* = 0.278655, \sigma = \sigma^*$, $(d_1, d_2) = (0.1, 0.1)$ falls in the region III of Figure 9(b), which is consistent with the case of Corollary 3(6), the pure Neimark-Sacker instability occurs, parasite and host populations exhibit periodic oscillatory behavior in two-dimensional space.

LS^* such that $1 - p(k_{l,s}^2) + q(k_{l,s}^2) = 0, q(k_{l,s}^2) = 1$, $M = \|\lambda_{1,2}(k_{1,1})\| = |\lambda_{3,4}(k_{l,s})| = \quad 1\ (\lambda_{3,4}(k_{l,s}) = -1)$. According to Corollary 3(9), a Neimark-Sacker-Flip-Flip bifurcation occurs, the number of parasites and hosts in two-dimensional space is very complex and can be regarded as a chaotic phenomenon, see Figures 26 and 27.

(e) When $d_1 = 0.25$ and $d_2 = 0.15$, (d_1, d_2) will fall in the region IV of Figure 9(b), which is consistent with the case of Corollary 3(10), the Neimark-Sacker-Turing instability occurs, parasite and host populations exhibit an unstable state in two-dimensional space, see Figure 28.

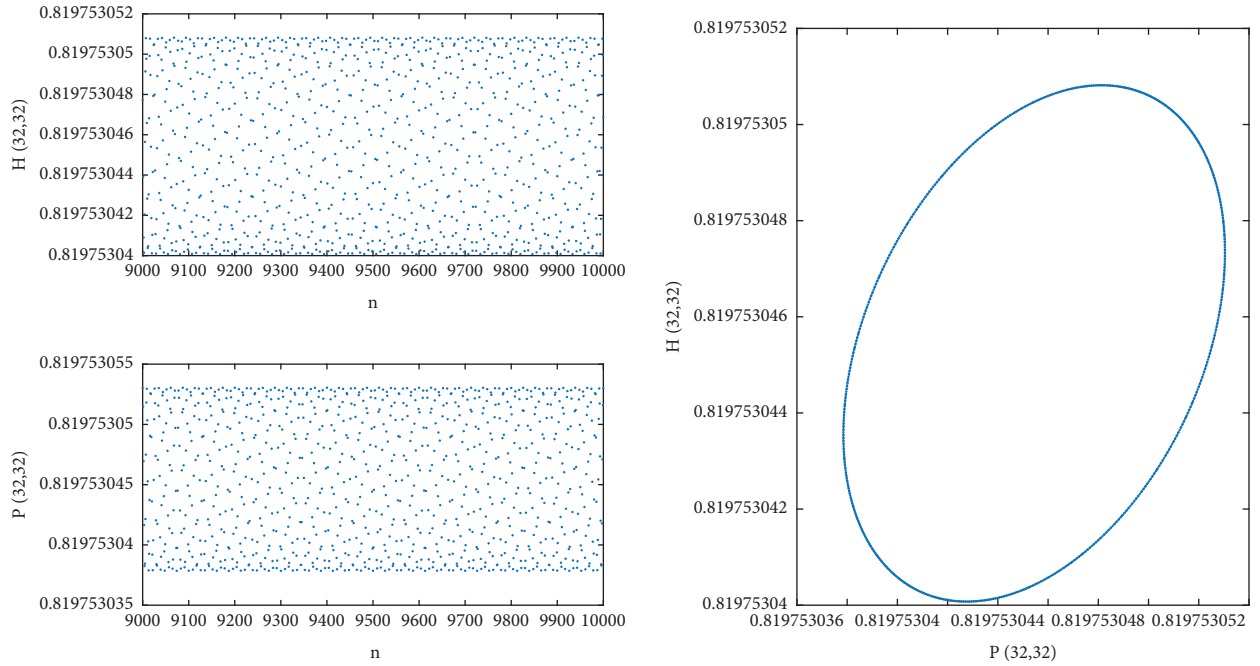

FIGURE 21: $R = 2, k = 1, \gamma = 0.8, \sigma^* = 0.278655, \sigma = \sigma^*, (d_1, d_2) = (0.1, 0.1)$ falls in the region III of Figure 9(b), which is consistent with the case of Corollary 3(6), the pure Neimark-Sacker instability occurs, parasite and host populations exhibit periodic oscillatory behavior.

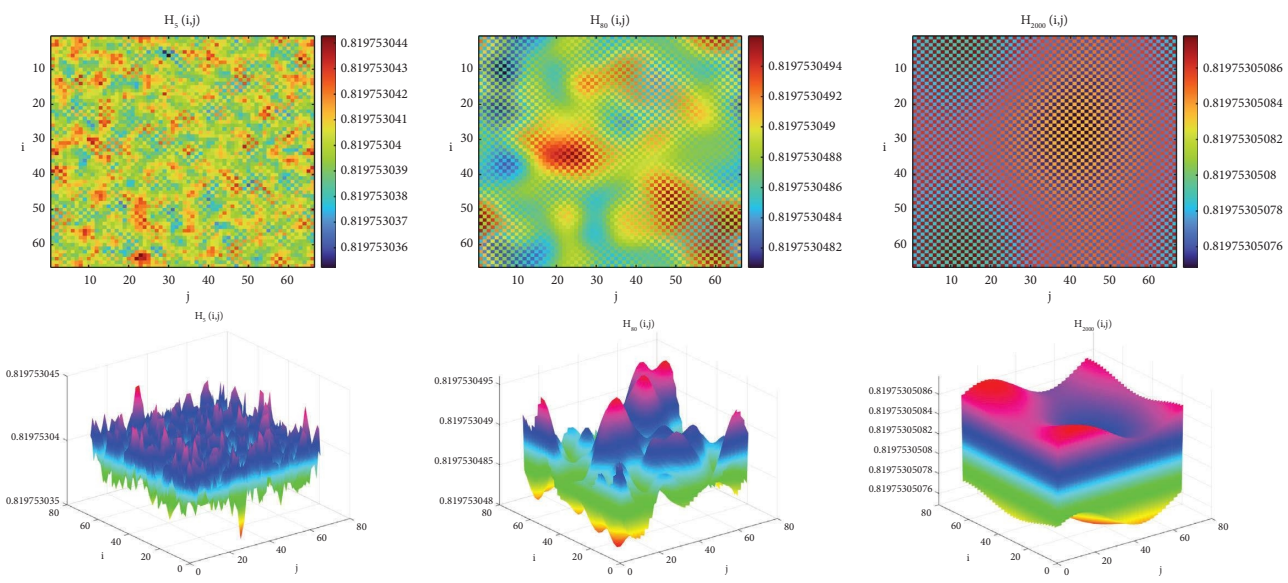

FIGURE 22: Continued.

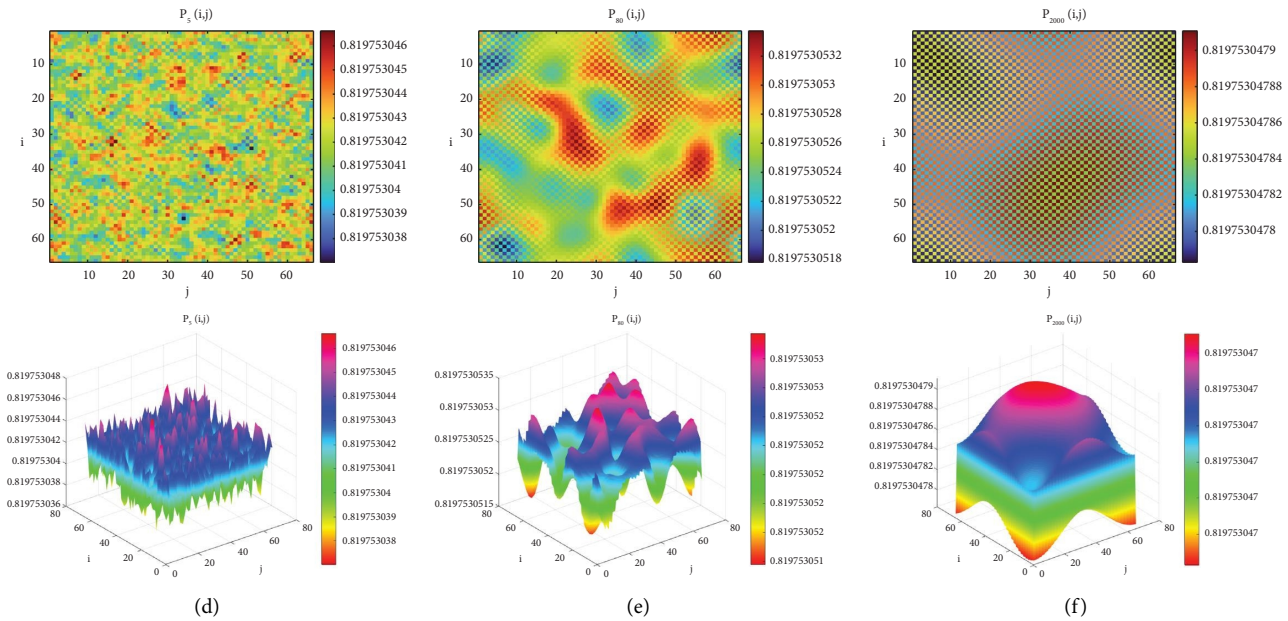

FIGURE 22: $R = 2, k = 1, \gamma = 0.8, \sigma^* = 0.278655, \sigma = \sigma^*, (d_1, d_2) = (0.3, 0.03125)$ falls at the junction of regions III and IV in Figure 9(b), which is consistent with the case of Corollary 3(7), a Neimark-Sacker-Flip bifurcation occurs, the number of parasites and hosts in two-dimensional space can show periodic doubling and periodic oscillation alternately.

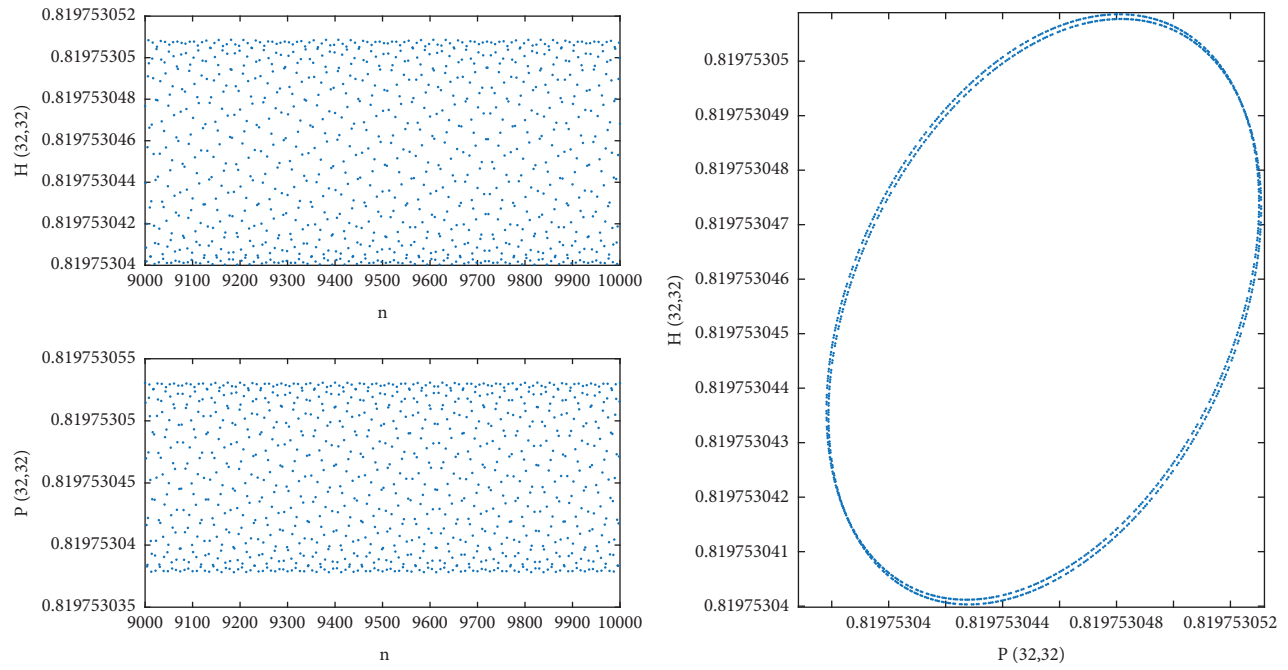

FIGURE 23: $R = 2, k = 1, \gamma = 0.8, \sigma^* = 0.278655, \sigma = \sigma^*, (d_1, d_2) = (0.3, 0.03125)$ falls at the junction of regions III and IV in Figure 9(b), which is consistent with the case of Corollary 3(7), a Neimark-Sacker-Flip bifurcation occurs, the number of parasites and hosts can show periodic doubling and periodic oscillation alternately.

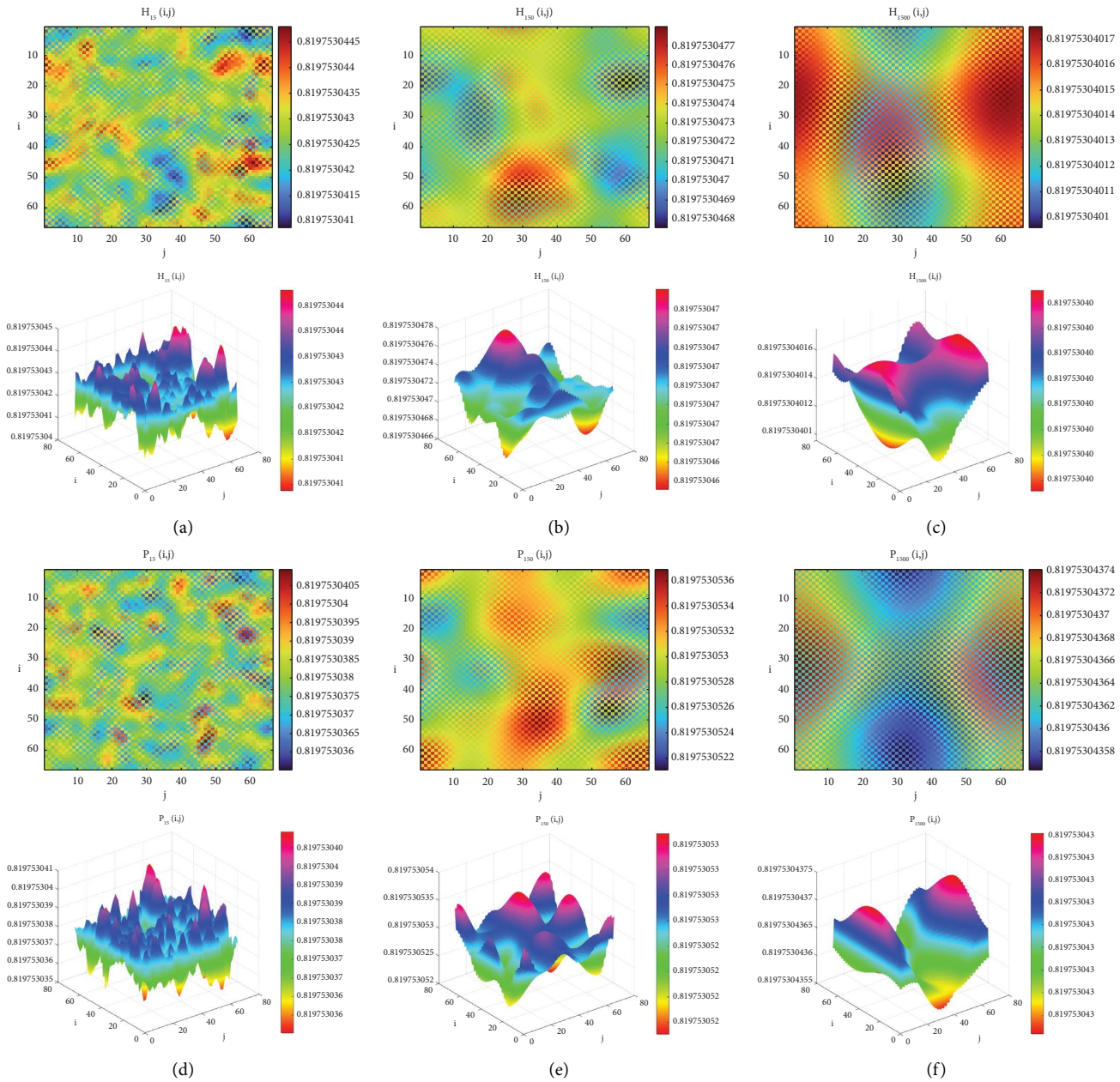

FIGURE 24: $R = 2, k = 1, \gamma = 0.8, \sigma^* = 0.278655, \sigma = \sigma^*, (d_1, d_2) = (0.2, 0.166667)$ falls at the junction of regions III and IV in Figure 9(b), which is consistent with the case of Corollary 3(8), a Neimark-Sacker-Neimark-Sacker bifurcation occurs, parasite and host populations generally exhibit periodic oscillatory behavior in two-dimensional space.

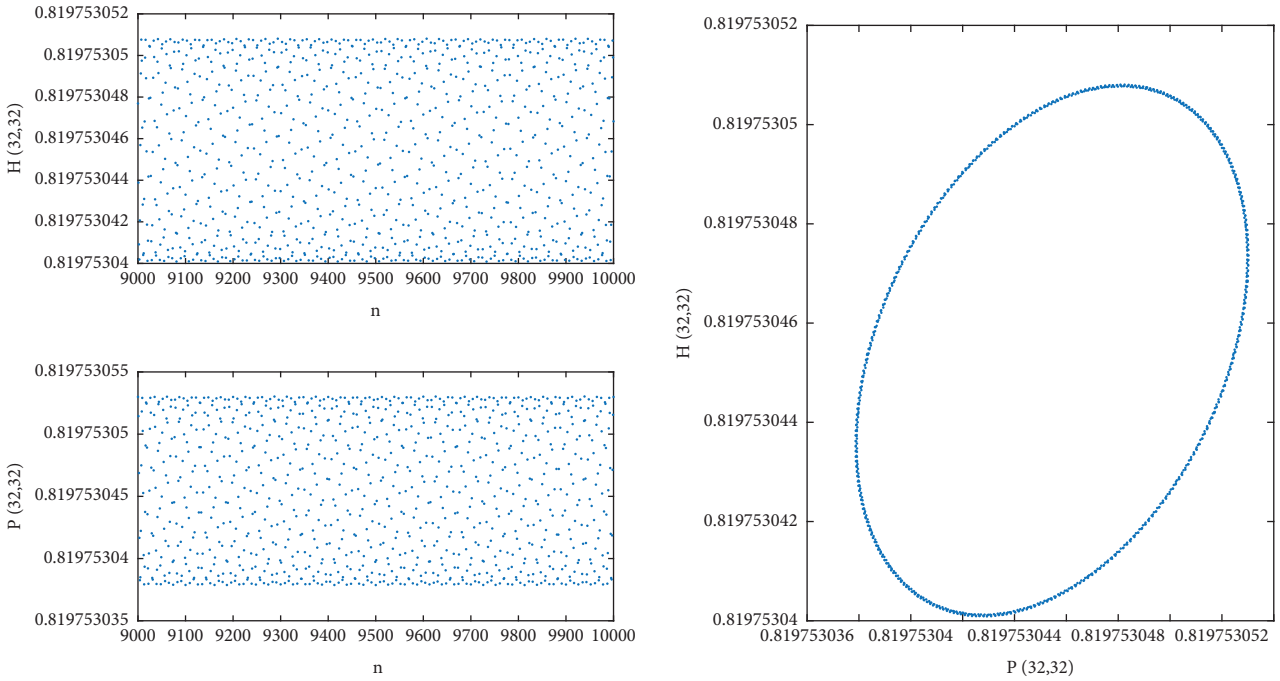

Figure 25: $R = 2, k = 1, \gamma = 0.8, \sigma^* = 0.278655, \sigma = \sigma^*, (d_1, d_2) = (0.2, 0.166667)$ falls at the junction of regions III and IV in Figure 9(b), which is consistent with the case of Corollary 3(8), a Neimark-Sacker-Neimark-Sacker bifurcation occurs, parasite and host populations generally exhibit periodic oscillatory behavior.

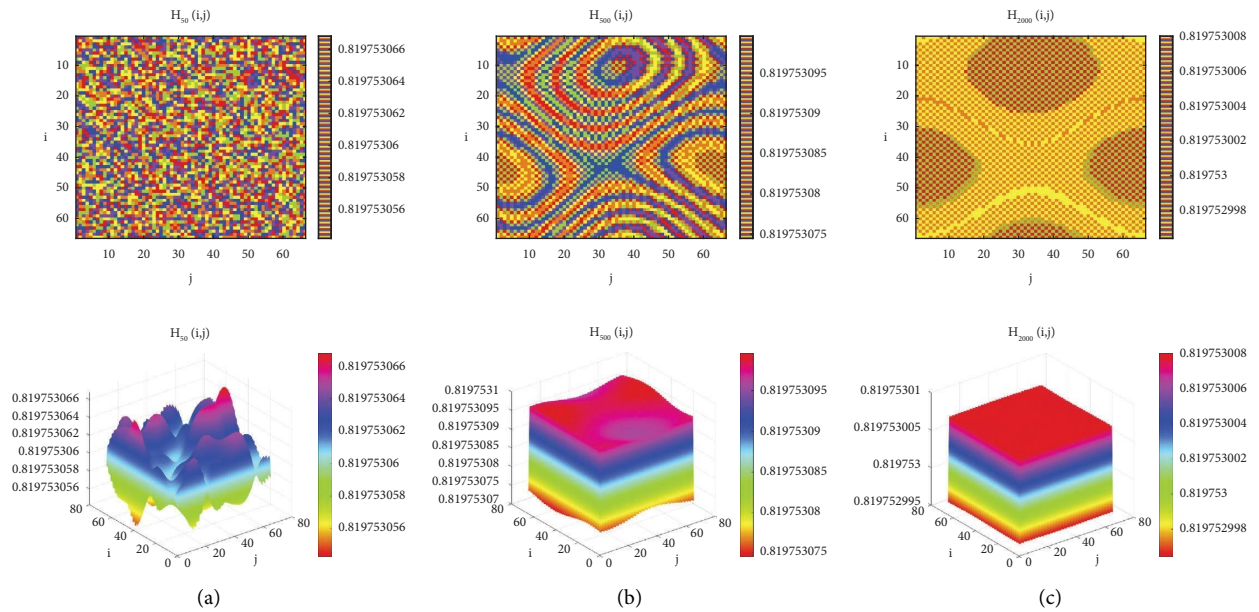

Figure 26: Continued.

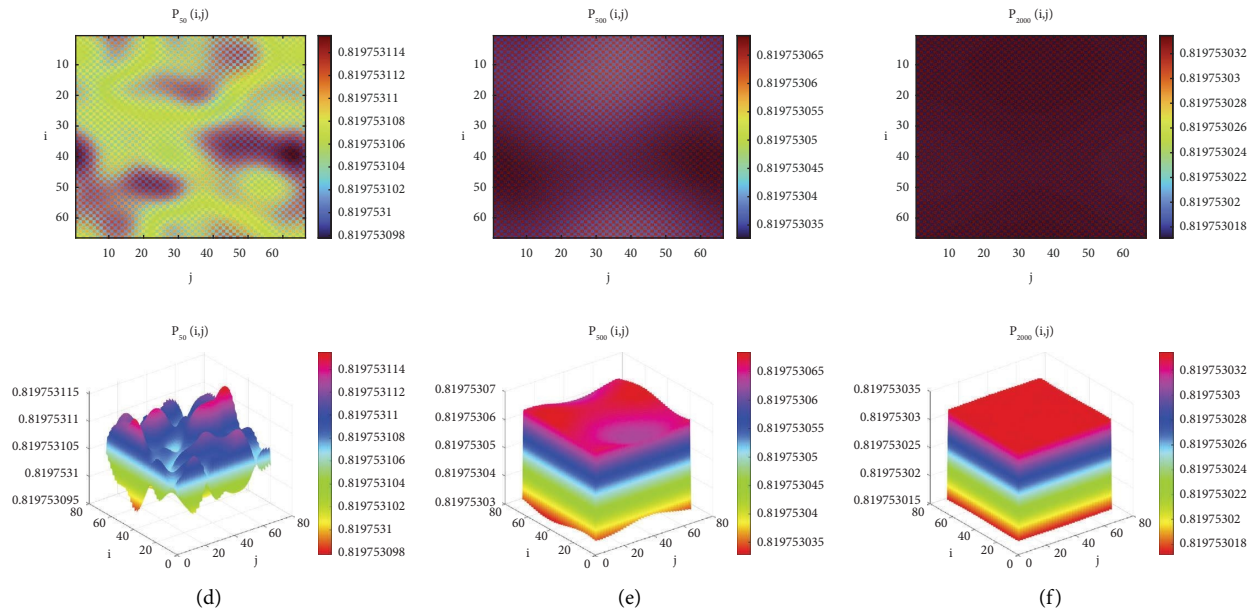

FIGURE 26: $R = 2, k = 1,\ \gamma = 0.8,\ \sigma^* = 0.278655,\ \sigma = \sigma^*,\ (d_1, d_2) = (0.161612, 0.275888)$ falls at the junction of regions III and IV in Figure 9(b), which is consistent with the case of Corollary 3(9), a Neimark-Sacker-Flip-Flip bifurcation occurs, the number of parasites and hosts in two-dimensional space is very complex and can be regarded as a chaotic phenomenon.

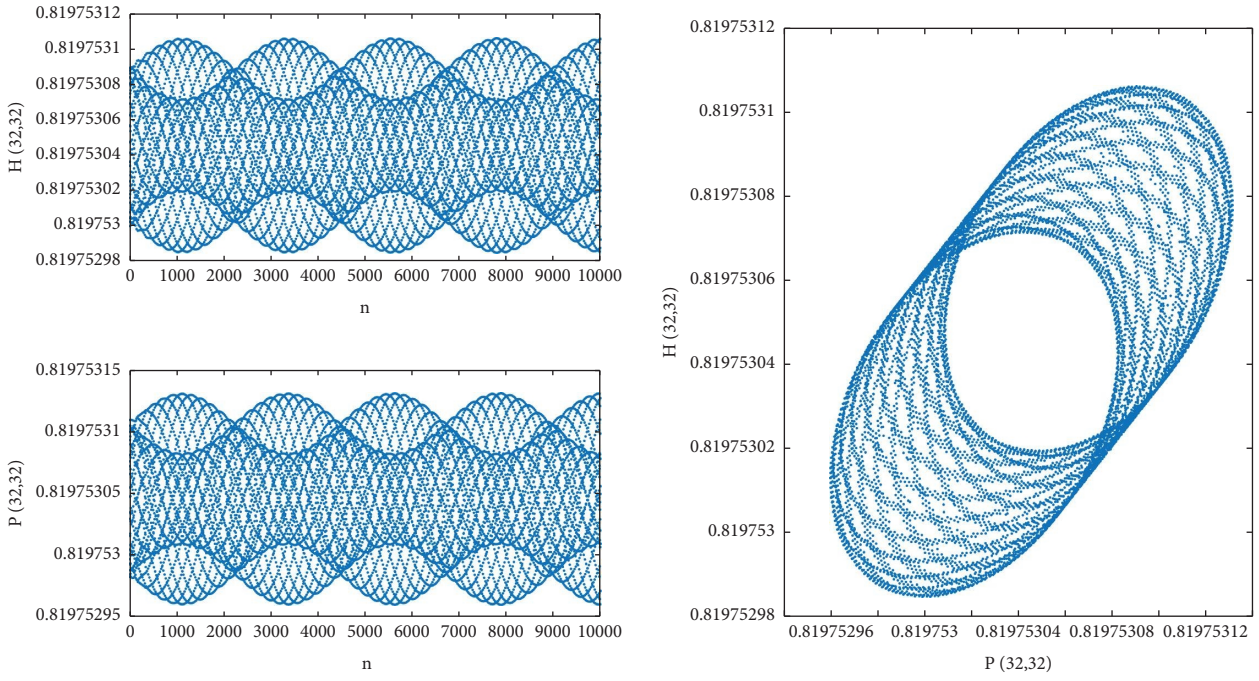

FIGURE 27: $R = 2, k = 1,\ \gamma = 0.8,\ \sigma^* = 0.278655,\ \sigma = \sigma^*,\ (d_1, d_2) = (0.161612, 0.275888)$ falls at the junction of regions III and IV in Figure 9(b), which is consistent with the case of Corollary 3(9), a Neimark-Sacker-Flip-Flip bifurcation occurs, the number of parasites and hosts is very complex and can be regarded as a chaotic phenomenon.

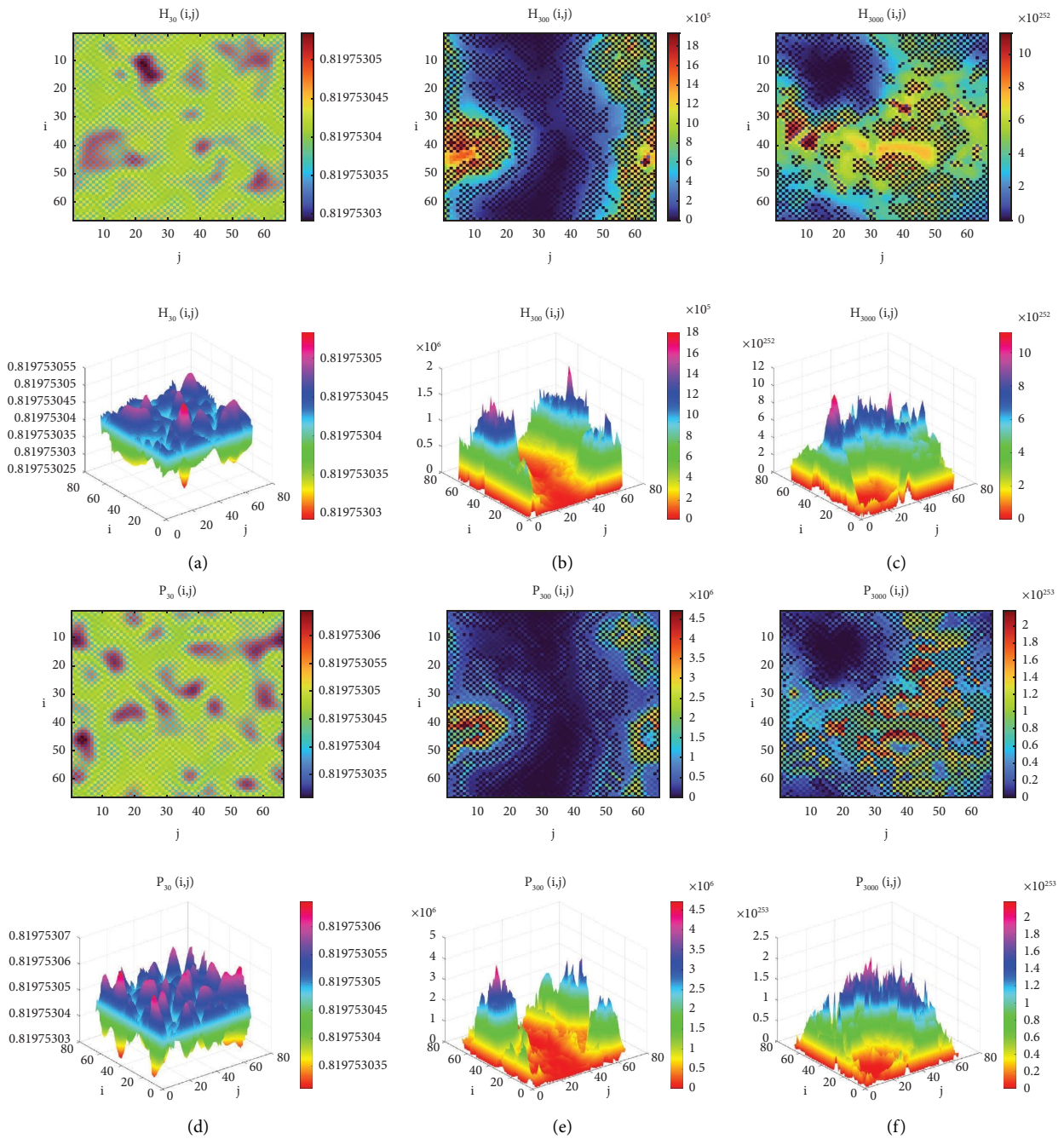

FIGURE 28: $R = 2, k = 1, \gamma = 0.8, \sigma^* = 0.278655, \sigma = \sigma^*, (d_1, d_2) = (0.25, 0.15)$ falls in the region IV of Figure 9(b), which is consistent with the case of Corollary 3(10), the Neimark-Sacker-Turing instability occurs, parasite and host populations exhibit an unstable state in two-dimensional space.

5. Summary

In this paper, we analyze the dynamical properties of a general time-space discrete host-parasitoid model with the periodic boundary conditions. We analyzed and obtained the asymptotically stable condition (Theorem 1), a Neimark-Sacker bifurcation condition (Theorem 2) for this general host-parasitoid model in the absence of diffusions and various instability conditions (Theorem 3) caused by diffusion-driven. Afterwards, we apply these obtained theoretical results to a modified Nicholson-Bailey model and obtained the corresponding corollaries (Corollaries 1–3). Finally, we performed numerical simulations of the modified Nicholson-Bailey model based on these corollaries (Figures 3, 4 and 10–28).

Numerical simulations show that hosts and parasitoids can exhibit complex spatiotemporal dynamics such as asymptotically stable (Figure 3), a Neimark-Sacker bifurcation (Figure 4) in the absence of diffusion and a homogeneous stationary (Figures 10 and 13), the pure Turing instability

(Figures 11 and 12), a Flip bifurcation (Figures 14 and 15), a Neimark-Sacker bifurcation (Figures 16 and 17), a 1 : 2 Resonance (Figures 18 and 19), the pure Neimark-Sacker instability (Figures 20 and 21), a Neimark-Sacker-Flip bifurcation (Figures 22 and 23), a Neimark-Sacker-Neimark-Sacker bifurcation (Figures 24 and 25), a Neimark-Sacker-Flip-Flip bifurcation (Figures 26 and 27), the Neimark-Sacker-Turing instability (21) by diffusion-driven. For the modified Nicholson-Bailey model, it is worth mentioning that it is possible for the eigenvalues of the Jacobi matrix B of system (30) to be equal to -1 due to the diffusion-driven, which cannot happen for the eigenvalues of the Jacobi matrix A of system (6) in the absence of diffusion. This can be shown specifically by the occurrence of a Flip bifurcation (Figures 14 and 15), a 1 : 2 Resonance (Figures 18 and 19), a Neimark-Sacker-Flip bifurcation (Figures 22 and 23) and a Neimark-Sacker-Flip-Flip bifurcation (Figures 26 and 27).

Finally, we have the following suggestions for possible future work: we can describe the system by using discrete time delay, for example, consider the delay of predator action on prey, we rewritten equation (1) as follows:

$$\begin{cases} H_{n+1} = RH_n f\left(RH_n, P_{n-m}\right), \\ P_{n+1} = kRH_n\left(1 - f\left(RH_n, P_{n-m}\right)\right), \end{cases} \tag{48}$$

where m is a positive integer, indicating the time delay. Interested readers can refer to reference [41]. We also hope to do further research and analysis on these high-dimensional bifurcations in the future to make our own contribution to biological control and biocontrol.

Data Availability

No underlying data was collected or produced in this study.

Conflicts of Interest

The authors declare that they have no conflicts of interest.

References

[1] M. Li, B. Han, L. Xu, and G. Zhang, "Spiral patterns near Turing instability in a discrete reaction diffusion system," *Chaos, Solitons and Fractals*, vol. 49, pp. 1–6, 2013.

[2] G. Zhang, R. Zhang, and Y. Yan, "The diffusion-driven instability and complexity for a single-handed discrete Fisher equation," *Applied Mathematics and Computation*, vol. 371, Article ID 124946, 2020.

[3] H. Zhang, T. Huang, L. Dai et al., "Regular and irregular vegetation pattern formation in semiarid regions: a study on discrete Klausmeier model," *Complexity*, vol. 2020, Article ID 2498073, 14 pages, 2020.

[4] W. Jiang, Q. An, and J. Shi, "Formulation of the normal form of Turing-Hopf bifurcation in partial functional differential equations," *Journal of Differential Equations*, vol. 268, no. 10, pp. 6067–6102, 2020.

[5] F. Yi, J. Wei, and J. Shi, "Bifurcation and spatiotemporal patterns in a homogeneous diffusive predator-prey system," *Journal of Differential Equations*, vol. 246, no. 5, pp. 1944–1977, 2009.

[6] Y. Song, H. Jiang, and Y. Yuan, "Turing-Hopf bifurcation in the reaction diffusion system with delay and application to a diffusive predator-prey model," *Journal of Applied Analysis and Computation*, vol. 9, no. 3, pp. 1132–1164, 2019.

[7] J. Wang and S. Liu, "Turing and Hopf bifurcation in a diffusive tumor-immune model," *Journal of Nonlinear Modeling and Analysis*, vol. 3, pp. 477–493, 2021.

[8] S. Xu and C. Zhang, "Spatiotemporal patterns induced by cross-diffusion on vegetation model," *AIMS Mathematics*, vol. 7, no. 8, pp. 14076–14098, 2022.

[9] H. Chen and C. Zhang, "Dynamic analysis of a Leslie-Gower-type predator-prey system with the fear effect and ratio-dependent Holling III functional response," *Nonlinear Analysis Modelling and Control*, vol. 27, no. 5, pp. 1–23, 2022.

[10] R. Muolo, M. Asllani, D. Fanelli, P. K. Maini, and T. Carletti, "Patterns of non-normality in networked systems," *Journal of Theoretical Biology*, vol. 480, pp. 81–91, 2019.

[11] Z. Li, Y. Song, and C. Wu, "Turing instability and Hopf bifurcation of a spatially discretized diffusive Brusselator model with zero-flux boundary conditions," *Nonlinear Dynamics*, vol. 111, 2022.

[12] S. Chen, J. Wei, and J. Yu, "Stationary patterns of a diffusive predator-prey model with Crowley-Martin functional response," *Nonlinear Analysis: Real World Applications*, vol. 39, pp. 33–57, 2018.

[13] X. Zhang and H. Zhu, "Dynamics and pattern formation in homogeneous diffusive predator-prey systems with predator interference or foraging facilitation," *Nonlinear Analysis: Real World Applications*, vol. 48, pp. 267–287, 2019.

[14] W. Jiang, H. Wang, and X. Cao, "Turing instability and Turing-Hopf bifurcation in diffusive schnakenberg systems with gene expression time delay," *Journal of Dynamics and Differential Equations*, vol. 31, no. 4, pp. 2223–2247, 2019.

[15] R. Su and C. Zhang, "Pattern dynamical behaviors of one type of Tree-Grass model with cross-diffusion," *International Journal of Bifurcation and Chaos*, vol. 32, no. 4, Article ID 2250051, 2022.

[16] L. Xu, J. Liu, and G. Zhang, "Pattern formation and parameter inversion for a discrete Lotka-Volterra cooperative system," *Chaos, Solitons and Fractals*, vol. 110, pp. 226–231, 2018.

[17] S. Ghorai, P. Chakraborty, S. Poria, and N. Bairagi, "Dispersal-induced pattern-forming instabilities in host-parasitoid metapopulations," *Nonlinear Dynamics*, vol. 100, no. 1, pp. 749–762, 2020.

[18] A. Q. Khan, "Supercritical Neimark-Sacker bifurcation of a discrete-time Nicholson-Bailey model," *Mathematical Methods in the Applied Sciences*, vol. 41, no. 12, pp. 4841–4852, 2018.

[19] M. H. Akrami and A. Atabaigi, "Dynamics and Neimark-Sacker bifurcation of a modified Nicholson-Bailey model," *Journal of Mathematical Extension*, vol. 16, 2021.

[20] A. Atabaigi and M. H. Akrami, "Dynamics and bifurcations of a host–parasite model," *International Journal of Biomathematics*, vol. 10, no. 06, Article ID 1750089, 2017.

[21] J. Bektesevic, V. Hadziabdic, S. Kalabušić, M. Mehuljic, and E. Pilav, "Dynamics of a class of host-parasitoid models with external stocking upon parasitoids," *Advances in Difference Equations*, vol. 2021, no. 1, 2021.

[22] M. Jervis, *Insects as Natural Enemies: A Practical Perspective*, Springer Science and Business Media, Berlin, Germany, 2007.

[23] W. Murdoch, C. Briggs, and R. Nisbet, *Consumer-Resouse Dynamics*, Princeton University Press, Princeton, NJ, USA, 2003.

[24] M. P. Hassell and G. C. Varley, "New inductive population model for insect parasites and its bearing on biological control," *Nature*, vol. 223, no. 5211, pp. 1133–1137, 1969.
[25] M. P. Hassell, "Host-parasitoid population dynamics," *Journal of Animal Ecology*, vol. 69, no. 4, pp. 543–566, 2000.
[26] A. J. Nicholson and V. A. Bailey, "The balance of animal populations.-part I," *Proceedings of the Zoological Society of London*, vol. 105, no. 3, pp. 551–598, 1935.
[27] A. Singh and B. Emerick, "Generalized stability conditions for host-parasitoid population dynamics: implications for biological control," *Ecological Modelling*, vol. 456, Article ID 109656, 2021.
[28] A. Q. Khan and M. N. Qureshi, "Dynamics of a modified Nicholson-Bailey host-parasitoid model," *Advances in Difference Equations*, vol. 2015, no. 1, 2015.
[29] Q. Din, W. Ishaque, M. A. Iqbal, and U. Saeed, "Modification of Nicholson-Bailey model under refuge effects with stability, bifurcation, and chaos control," *Journal of Vibration and Control*, vol. 28, no. 23-24, pp. 3524–3538, 2021.
[30] G. Livadiotis, L. Assas, B. Dennis, S. Elaydi, and E. Kwessi, "A discrete-time host-parasitoid model with an Allee effect," *Journal of Biological Dynamics*, vol. 9, no. 1, pp. 34–51, 2015.
[31] A. Ozlem, "Dynamical consequences and stability analysis of a new host-parasitoid model," *General Mathematics Notes*, vol. 27, 2015.
[32] Q. Din, "Global stability and Neimark-Sacker bifurcation of a host-parasitoid model," *International Journal of Systems Science*, vol. 48, no. 6, pp. 1194–1202, 2017.
[33] X. Ma, Q. Din, M. Rafaqat, N. Javaid, and Y. Feng, "A density-dependent host-parasitoid model with stability, bifurcation and chaos control," *Mathematics*, vol. 8, no. 4, 2020.
[34] Q. Din and M. I. Khan, "A discrete-time model for consumer-resource interaction with stability, bifurcation and chaos control," *Qualitative Theory of Dynamical Systems*, vol. 20, no. 2, pp. 56–35, 2021.
[35] A. Singh, W. W. Murdoch, and R. M. Nisbet, "Skewed attacks, stability, and host suppression," *Ecology*, vol. 90, no. 6, pp. 1679–1686, 2009.
[36] M. P. Hassell, *The Spatial and Temporal Dynamics of Host Parasitoid Interactions*, Oxford University Press, Oxford, UK, 2000.
[37] W. S. Gurney and R. M. Nisbet, *Ecological Dynamics*, Oxford University Press, Oxford, UK, 1998.
[38] K. Marcinko and M. Kot, "A comparative analysis of host-parasitoid models with density dependence preceding parasitism," *Journal of Biological Dynamics*, vol. 14, no. 1, pp. 479–514, 2020.
[39] S. J. Schreiber, "Host-parasitoid dynamics of a generalized Thompson model," *Journal of Mathematical Biology*, vol. 52, no. 6, pp. 719–732, 2006.
[40] L. Bai and G. Zhang, "Nontrivial solutions for a nonlinear discrete elliptic equation with periodic boundary conditions," *Applied Mathematics and Computation*, vol. 210, no. 2, pp. 321–333, 2009.
[41] W. Li and X. Y. Li, "Neimark-Sacker bifurcation of a semi-discrete hematopoiesis model," *Journal of Applied Analysis & Computation*, vol. 8, no. 6, pp. 1679–1693, 2018.